# Measuring freshwater aquatic ecosystems: The need for a hyperspectral global mapping satellite mission

CrossMark

Erin Lee Hestir [a,b,*], Vittorio E. Brando [a,c], Mariano Bresciani [c], Claudia Giardino [c], Erica Matta [c], Paolo Villa [c], Arnold G. Dekker [a]

[a] Commonwealth Scientific & Industrial Research Organization (CSIRO), Canberra, Australia
[b] Department of Marine, Earth & Atmospheric Sciences, NC State University, Raleigh, USA
[c] Institute for Electromagnetic Sensing of the Environment (CNR-IREA), Milano, Italy

## ARTICLE INFO

## ABSTRACT

Freshwater ecosystems underpin global water and food security, yet are some of the most endangered ecosystems in the world because they are particularly vulnerable to land management change and climate variability. The US National Research Council's guidance to NASA regarding missions for the coming decade includes a polar orbiting, global mapping hyperspectral satellite remote sensing mission, the Hyperspectral Infrared Imager (HyspIRI), to make quantitative measurements of ecosystem change. Traditionally, freshwater ecosystems have been challenging to measure with satellite remote sensing because they are small and spatially complex, require high fidelity spectroradiometry, and are best described with biophysical variables derived from high spectral resolution data. In this study, we evaluate the contribution of a hyperspectral global mapping satellite mission to measuring freshwater ecosystems. We demonstrate the need for such a mission, and evaluate the suitability and gaps, through an examination of the measurement resolution issues impacting freshwater ecosystem measurements (spatial, temporal, spectral and radiometric). These are exemplified through three case studies that use remote sensing to characterize a component of freshwater ecosystems that drive primary productivity. The high radiometric quality proposed for the HyspIRI mission makes it uniquely well designed for measuring freshwater ecosystems accurately at moderate to high spatial resolutions. The spatial and spectral resolutions of the HyspIRI mission are well suited for the retrieval of multiple biophysical variables, such as phycocyanin and chlorophyll-a. The effective temporal resolution is suitable for characterizing growing season wetland phenology in temperate regions, but may not be appropriate for tracking algal bloom dynamics, or ecosystem responses to extreme events in monsoonal regions. Global mapping missions provide the systematic, repeated measurements necessary to measure the drivers of freshwater biodiversity change. Archival global mapping missions with open access and free data policies increase end user uptake globally. Overall, an archival, hyperspectral global mapping mission uniquely meets the measurement requirements of multiple end users for freshwater ecosystem science and management.

## 1. Introduction

### 1.1. Freshwater ecosystems in the Anthropocene

Increasing pressure for human water, food and energy security make understanding freshwater ecosystem processes and managing sustainable ecosystem services critical. Freshwater is a fundamental resource for human life, and the services provided by surface freshwater ecosystems underpin global water security, food security and economic productivity (Hanjra & Qureshi, 2010). Freshwater ecosystems occur in freshwater systems including lakes, ponds, streams and rivers, and in the wetlands, marshes, swamps and bogs associated with these water bodies. Freshwater systems provide multiple services to both humans and the environment, including 1) provisioning water for consumption, energy, and transportation; 2) cultural amenities such as recreation, tourism and religious significance; 3) maintaining water quality, flood and erosion control; and 4) supporting biodiversity and ecosystem function such as nutrient and carbon cycling and primary production (Aylward et al., 2005).

The intensifying exploitation of freshwater resources to meet the water, energy and food needs of a rapidly growing global population often places biodiversity and other ecosystem functions at risk. The degradation of these services is exacerbated by climate change and variability. Surface freshwaters are among the most anthropogenically modified ecosystems on Earth (Carpenter, Stanley, & Vander Zanden,

2011), and are exceptionally vulnerable to climate change (Woodward, Perkins, & Brown, 2010). Although freshwater systems occupy a relatively small portion of the Earth's surface (~2–3%; Downing et al., 2006; Raymond et al., 2013), freshwater ecosystems have a disproportionate role in driving global biodiversity and ecological function. Freshwater ecosystems support 10% of the world's animal species, and nearly 35% of all vertebrate species (Stendera et al., 2012). Unfortunately, freshwater ecosystems have the highest rates of biodiversity loss globally, and may be the most endangered ecosystems in the world (Dudgeon et al., 2006).

Freshwater ecosystems are also increasingly recognized as an important factor in the global carbon cycle. Carbon emissions from surface inland waters are estimated to be on the same order of magnitude as carbon emissions from deforestation or carbon uptake from oceans (Tranvik et al., 2009). Yet inland waters are poorly accounted for in global estimates of terrestrial net primary production (Raymond et al., 2013). Wetlands are widely recognized as one of the most important sources of global methane emissions, but also sequester large amounts of carbon dioxide in the soils. The relative role of freshwater ecosystems in the carbon cycle and how that role will change with increasing pressure from human activity and changing climate is poorly understood and requires significant study (e.g., Bridgham, Moore, Richardson, & Roulet, 2014; Mitsch et al., 2013).

### 1.2. Observation needs

To improve understanding of global freshwater responses to multiple stressors, valid, standardized and accurate data are needed. In collecting data in the field, there are logistical, operational and financial considerations that usually impede freshwater ecosystem measurements. *In situ* measurements and monitoring provide detailed information pertinent to understanding key ecosystem characteristics, forming the basis of long term monitoring records needed to assess status and identify trends. Unfortunately, in situ approaches are limited to point-based representations of complex and dynamic systems. Furthermore, *in situ* measurements in freshwater systems are also limited by logistics such as access, cost and timing, which all restrict systematicity. Satellite remote sensing can complement *in situ* freshwater ecosystem sampling.

The potential of satellite remote sensing for freshwater inventory and monitoring has long been recognized by the scientific community; optical satellite datasets have been used to detect freshwater systems for decades (e.g., Carpenter & Carpenter, 1983; Lulla, 1983; Strong, 1974), as have active remote sensing datasets (Melack, 2004). Stand-alone radar data or radar used in conjunction with optical remote sensing data have been particularly useful for wetland and flood plain detection (Alsdorf et al., 2000; Henderson & Lewis, 2008; Hess, Melack, Novo, Barbosa, & Gastil, 2003; Silva, Costa, & Melack, 2010), lake detection, surface and volume estimates (Crétaux et al., 2011; Strozzi, Wiesmann, Kääb, Joshi, & Mool, 2012). Traditionally, however, satellite remote sensing of freshwater systems has been limited by sensor technology; current and past missions have not provided the measurement resolutions needed to fully resolve freshwater ecosystem properties and processes.

Optical satellite remote sensing of Earth's ecosystems has helped to transform our understanding of ecosystem change (Cohen & Goward, 2004; Wulder, Masek, Cohen, Loveland, & Woodcock, 2012). High spectral resolution (hyperspectral) remote sensing, or imaging spectroscopy, provides measurements across hundreds of discrete bands, forming a contiguous spectrum that enables detection and identification of earth surface materials, which makes quantitative measurements of ecosystem properties and processes surpassing other remote sensing modalities (Bioucas-Dias et al., 2013; Green et al., 1998; Ustin, Roberts, Gamon, Asner, & Green, 2004). Archival, polar orbiting, global mapping satellite missions make systematic measurements over years to decades, providing a time series of consistently measured data to assess system condition, identify change, and understand process for a limited, but important suite of biophysical variables.

Freshwater systems may be small and spatially complex, requiring moderate to small pixel sizes. Discriminating wetland vegetation requires moderate to high spatial and spectral resolutions in both visible and shortwave infrared regions (Hestir et al., 2008). Inferring ecosystem process such as watershed runoff, environmental flows, lake currents and stratification, and inundation processes that drive habitat connectivity, sediment and nutrient discharge, algal blooms, and wetland greenhouse gas emissions from space requires both high spatial and temporal resolutions (Kutser, Metsamaa, Strömbeck, & Vahtmäe, 2006; Song, Xu, Tian, & Wang, 2009). Measuring water column conditions requires satellite measurements to have high spectral resolution and the sensitivity to resolve small changes in water-leaving radiance relative to the noise of the sensor and the atmosphere (i.e., high radiometric resolution and high signal to noise ratio; Hu et al., 2012). Several reviews published over the past decades have summarized the applications, potential and limitations of satellite remote sensing for freshwater systems based on these resolution limitations (Adam, Mutanga, & Rugege, 2010; Carbonneau & Piegay, 2012; Dekker & Hestir, 2012; Heumann, 2011; Klemas, 2013a,b, 2014; Matthews, 2011; Mertes, 2002; Odermatt, Gitelson, Brando, & Schaepman, 2012; Ozesmi & Bauer, 2002).

### 1.3. The Hyperspectral Infrared Imager (HyspIRI) mission

The United States National Research Council (US NRC) highlights the need for a global mapping satellite mission that deploys an imaging spectrometer to make much needed global observations of ecosystem change (National Research Council, 2007). The US NRC's guidance to NASA recommends the development of the Hyperspectral Infrared Imager (HyspIRI) to address this need. The proposed mission will make optical measurements in over 200 bands in the visible, near and shortwave infrared, and will have multiple thermal infrared bands. HyspIRI is planned to have an equatorial revisit time of ~19 days, with a 60 m pixel resolution (Devred et al., 2013). To the best of our knowledge, there is no other current or planned mission that could deliver archival, regularly repeated measurements with the high spectral and spatial resolutions needed to address freshwater ecosystem science and management challenges. In this study, we evaluate the potential contribution of a hyperspectral global mapping satellite mission to measuring freshwater ecosystems, focusing on passive optical remote sensing in the visible, near and shortwave infrared regions. We demonstrate the need for such a mission, and evaluate the suitability and gaps of such a mission through an examination of the measurement resolution (spatial, temporal, spectral and radiometric), exemplified through three case studies that use remote sensing to characterize a component of freshwater ecosystem primary production.

## 2. Observing freshwater systems from space

### 2.1. Freshwater ecology in remote sensing literature

As sensor technologies have improved both in measurement fidelity and spatial and spectral resolutions, the application of remote sensing to freshwater systems has also increased. Since 2000, the portion of aquatic applications in remote sensing publications has shown a significant increasing trend of 4% of the mean portion of remote sensing publications per year (Mann–Kendall test for trend: $\tau = 0.58$, $p = 0.004$; Fig. 1).

### 2.2. Freshwater resource management and satellite remote sensing products

Based on a survey of US Environmental Protection Agency personnel, Schaeffer et al. (2013) described the primary barriers to water quality managers adopting satellite products. These include 1) actual and perceived cost, both in terms of cost of data and cost for accessing
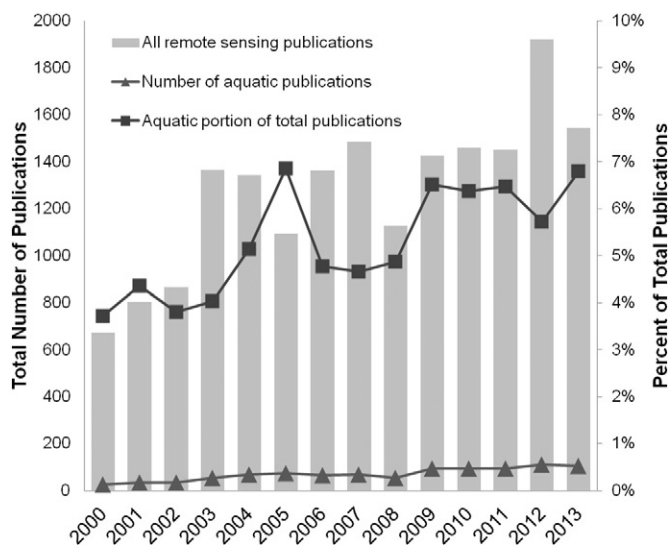
**Fig. 1.** Total number of publications by year (light gray bars) from a Web of Science database search for "remote sensing" as a topic, under the research area "remote sensing" and the research domain "science and technology." The portion of aquatic remote sensing publications was determined by querying this database return for the topics "aquatic," "lake," or "wetlands." There is a significant increasing trend of 4% of the mean portion of publications per year.

personnel with expertise in remote sensing; 2) confidence in product accuracy; 3) satellite data continuity, and 4) programmatic support for training personnel and new software applications. Despite the presence of these barriers, there are clear examples of high spectral resolution remote sensing being applied to management of water quality (e.g., Bresciani, Stroppiana, Odermatt, Morabito, & Giardino, 2011), wetlands (e.g., Rebelo, Finlayson, & Nagabhatla, 2009), and aquatic invasive alien species (e.g., Santos et al., 2009). While high spectral resolution data cannot address all of the barriers to management adoption of

satellite products, algorithms for retrieving the biophysical properties of freshwater ecosystems are mature, and can support high accuracy products at low cost to the end-user. Satellite and hyperspectral remote sensing have long been used for wetland classification and evaluation (e.g., Artigas & Yang, 2007; Hardisky, Gross, & Klemas, 1986; Lulla, 1983; Peñuelas, Gamon, Griffin, & Field, 1993; Ramsey & Rangoonwala, 2011; Schmidt & Skidmore, 2003; Zomer, Trabucco, & Ustin, 2009). And while algorithms for freshwater water quality have been successfully applied to satellite and hyperspectral remote sensing data for decades (e.g., Dekker, Malthus, & Goddijn, 1992; Dekker, Malthus, Wijen, & Seyhan, 1992; Hoogenboom, Dekker & Althius, 1998; Hoogenboom, Dekker & De Haan, 1998; Kutser, Herlevi, Kallio, & Arst, 2001; Pierson & Strömbeck, 2001; Strong, 1974), standard water quality products are mainly limited to ocean color products due to limitations imposed primarily by sensor characteristics, which are discussed below in the sections that follow.

### 2.2.1. Measuring freshwater ecosystem biophysical properties

Biophysical properties estimable from passive optical remote sensing are summarized in Table 1. Several reviews have been published recently that describe and evaluate algorithms for wetland detection and ecological evaluation (Adam et al., 2010; Klemas, 2011, 2013a,b, 2014; Mertes, 2002; Ozesmi & Bauer, 2002; Rundquist, Narumalani, & Narayanan, 2001; Silva, Costa, Melack, & Novo, 2008), and water quality (Blondeau-Patissier, Gower, Dekker, Phinn, & Brando, 2014; Devred et al., 2013; Kutser, 2009; Matthews, 2011; Odermatt et al., 2012; Ogashawara, Mishra, Mishra, Curtarelli, & Stech, 2013; Zhu et al., 2014). We refer readers to these reviews and references therein for a more complete description and evaluation of published algorithms.

A common thread among these reviews is that the algorithms that perform best are those that exploit hyperspectral data, because these datasets have narrow spectral bands in positions that focus on key biophysical properties of wetlands and the water column. HyspIRI will provide the narrow bands needed to make most of the biophysical estimates. For instance, detecting plant or phytoplankton species may be

**Table 1**
Biophysical properties estimable from passive optical remote sensing.

| Biophysical properties | Example references |
|---|---|
| Plant canopy (riparian, emergent, floating and submerged) | |
|   Plant species and distribution | Giardino, Bartoli, Candiani, Bresciani and Pellegrini (2007a), Hestir et al. (2012), Hestir et al. (2008), Khanna, Santos, Hestir, and Ustin (2012), Khanna et al. (2011), Underwood et al. (2006), and Zomer et al. (2009) |
|   Plant functional type | Dronova et al. (2012), Santos et al. (2012), and Ustin and Gamon (2010) |
|   Chlorophyll-a (CHL) | Gitelson and Merzlyak (1996) and Richardson, Duigan, and Berlyn (2002) |
|   Other photosynthetic & accessory pigments | Peñuelas et al. (1993) and Sims and Gamon (2002) |
|   Foliar chemistry | LaCapra, Melack, Gastil, and Valeriano (1996), Peñuelas et al. (1993), Ustin (2013), and Ustin et al. (2009) |
|   Photosynthetic pathways | Garbulsky, Peñuelas, Gamon, Inoue, and Filella (2011), Peñuelas et al. (1993), and Santos et al. (2012) |
|   Phenology and stress | Andrew and Ustin (2009), Dronova, Gong, and Wang (2011), and Khanna et al. (2012) |
|   Biomass | Byrd et al. (2014)[a] |
|   Carbon flux | Garbulsky et al. (2011)[a] |
| Water Column | |
|   Chlorophyll-a (CHL) | Gitelson et al. (2008), Gons, Auer, and Effler (2008), Matthews (2011)[a], and Odermatt et al. (2012)[a] |
|   Other photosynthetic & accessory pigments | Gons et al. (2005) and Simis et al. (2005) |
|   Phytoplankton functional type (PFT) | Devred et al. (2013)[a] |
|   Harmful algal blooms | Kutser (2009)[a], Matthews (2011)[a], and Odermatt et al. (2012)[a] |
|   Water surface extent | Amarnath (2014) and Vanderbilt et al. (2007) |
|   Water depth (bathymetry), channel morphology & benthic habitat | Legleiter, Roberts, Marcus, and Fonstad (2004) and Legleiter and Roberts (2005, 2009) |
|   Total suspended matter (TSM) | Devred et al. (2013)[a], Matthews (2011)[a], and Odermatt et al. (2012)[a] |
|   Suspended sediment concentration (SSC) | Bowers and Binding (2006), Doxoran, Froidefond, Lavender, and Castaing (2002), and Mertes (2002) |
|   Non-algal particulate matter/tripton (TR) | Devred et al. (2013)[a], Matthews (2011)[a], and Odermatt et al. (2012)[a] |
|   Suspended inorganic particulate matter (SPIM) | Devred et al. (2013)[a], Matthews (2011)[a], and Odermatt et al. (2012)[a] |
|   Colored dissolved organic matter (CDOM) | Matthews (2011)[a], Odermatt et al. (2012)[a], and Zhu et al. (2014)[a] |
|   Dissolved organic carbon (DOC) | Kutser et al. (2005), Giardino, Brando et al. (2007), and Hestir, Brando, Campbell, Dekker, and Malthus (2015) |
|   Vertical attenuation coefficient (Kd) | Devred et al. (2013)[a] and Odermatt et al. (2012)[a] |
|   Secchi disk depth/turbidity | Giardino, Brando et al. (2007), Kutser et al. (2001), Nelson, Soranno, Cheruvelil, Batzli, and Skole (2003), and Thiemann and Kaufmann (2002) |
|   Sediment, carbon and nutrient loads, Organic & inorganic micro-pollutants, and dissolved oxygen | Bjerklie, Lawrence Dingman, Vorosmarty, Bolster, and Congalton (2003), Brodie et al. (2010), Del Castillo and Miller (2008), Mertes (2002), Mertes and Warrick (2001), and Muller, DÉCamps, and Dobson (1993) |

[a] Indicates a recent review or study with useful references contained within.

difficult, even with hyperspectral data. However, species with similar function have similar physiology in terms of pigment composition (for plants and phytoplankton) and canopy structure (for plants). Therefore, the species will have spectral similarities that allow discrimination of functional types (Nair et al., 2008; Ustin & Gamon, 2010). Conversely, by understanding this process, it is possible to estimate biodiversity based on spectral diversity in plant canopies (Carlson, Asner, Hughes, Ostertag, & Martin, 2007; Rocchini et al., 2010) and in phytoplankton (Stomp et al., 2004; Striebel, Behl, Diehl, & Stibor, 2009), even if taxonomic identification is not achievable. However, high fidelity, high spectral and high spatial resolution data are required to resolve spectral diversity in order to make best estimates of biodiversity (Rocchini et al., 2010). While HyspIRI will provide the spectral resolution, at 60 m it may not provide the spatial resolution to distinguish spectral diversity in patchy, heterogeneous wetland canopies or swirls of phytoplankton colonies.

High spectral resolution data is also optimal for estimating water column and benthic biophysical properties. Narrow band, high spectral resolution data enable physics-based radiative transfer modeling approaches to quantitatively retrieve multiple water column constituents of interest (e.g., phycocyanin, chlorophyll-a, suspended mater, CDOM, phytoplankton functional types, water depth and benthic composition; Devred et al., 2013). In inland waters the concentrations of the optically active components of the water column (suspended matter, CDOM, and phytoplankton pigments) vary by orders of magnitude, and may co-vary or vary independently depending on the source and composition of the suspended and dissolved materials (Dekker, Malthus, & Goddijn, 1992; Dekker, Malthus, Wijen, & Seyhan, 1992). Further, the absorption features of in-water optically active constituents vary in depth, width, and location and may overlap in the reflectance signal (Ampe et al., 2014), creating confounding effects when trying to isolate any one biophysical parameter. For example, high CDOM concentrations may cause traditional empirical CHL algorithms to retrieve spurious CHL concentrations (Siegel, Maritorena, Nelson, Behrenfeld, & McClain, 2005), and multispectral (Landsat) detections of cyanobacteria blooms in Lake Erie by Vincent et al. (2004) were likely a result of phycocyanin correlating with a lurking variable such as turbidity, since Landsat lacks the necessary spectral bands to measure the diagnostic pigment phycocyanin (Kutser, 2009; Matthews, 2011). We elaborate on spectral resolution in the section that follows.
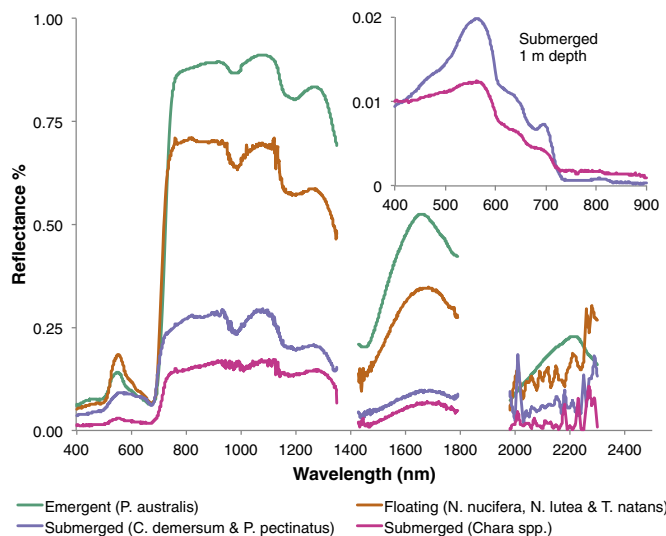
### 2.3. Spectral resolution

High spectral resolution data provides more spectral bands needed to unmix a greater number of endmembers (Schaepman et al., 2009), a common problem in freshwater ecosystems which tend to be spatially complex and spectrally heterogeneous at the 60 m pixel scale. For vegetation canopies, the high spatial and phenological variability of wetland/aquatic macrophytes necessitates high spectral resolution data to adequately discriminate communities (Klemas, 2013a), measure biochemical features (Ustin et al., 2004), and allows the potential for more sophisticated spectral unmixing models (e.g., Dennison & Roberts, 2003). For the water column, high spectral resolution data are needed to retrieve multiple optical water quality variables and to distinguish water column properties from the signal from the bottom in optically shallow areas.

Fig. 2 shows the reflectance spectra of four different aquatic macrophyte communities: emergent perennial common reed, *Phragmites australis*; floating leaved lotus (*Nelumbo nucifera*) and water chestnut (*Trapa natans*); submerged rooted sago pondweed (*Potamogeton pectinatus*) and free floating submerged coontail (*Ceratophyllum demersum*); and submerged algae chara (*Chara* spp.). The reflectance spectra of those communities were all measured above water. The inset graph in Fig. 2 shows the surface reflectance of the submerged species (coontail and sago in purple, and algae in pink) when submersed under 1 m of water with CHL concentration 0.8 mg m$^{-3}$, TSM concentration 0.7 g m$^{-3}$, and CDOM$_{(440)}$ absorption 0.2 m$^{-1}$. As the water column depth over submerged vegetation increases, the influence of the absorbing and scattering properties of the water column increases, changing the submerged vegetation signal (Fig. 2 inset; Hestir et al., 2008).

All regions of the spectrum (visible, near infrared, and shortwave infrared) have been shown to be important in discriminating different life forms of aquatic macrophytes (e.g., submerged, floating, and emergent) (e.g., Becker, Lusch, & Qi, 2007; Hestir, Greenberg, & Ustin, 2012; Khanna, Santos, Ustin, & Haverkamp, 2011). For species-level detection, the visible region is the most useful for submerged vegetation species (Santos, Hestir, Khanna, & Ustin, 2012), and the near and shortwave infrared regions are particularly useful for discriminating submerged vegetation from emergent and floating vegetation and species-level detection of floating and emergent macrophytes (Hestir et al., 2008; Hestir et al., 2012; Khanna et al., 2011; Rosso, Ustin, & Hastings, 2005).

Ustin et al. (2004) recommend high spectral resolution across the full 400–2500 nm spectrum for full quantitative estimates of vegetation biochemical composition. For vegetation, the strong absorption of light between 400 and 700 nm is primarily a function of photosynthetic pigments, and the high reflectance in the near-infrared (700–1100 nm) is dominated by multiple scattering of photons in the leaves and canopy, absorption by water, and minimal biochemical absorption. Reflectance in the shortwave infrared is dominated by water absorption, and absorption by leaf carbon compounds such as cellulose and lignin and other biochemicals such as nitrogen (Ustin et al., 2004).

High spectral resolution data also enable calculation of narrow band indices commonly used to identify spectral features that are then used for aquatic macrophyte detection, or correlated to vegetation biochemical and biophysical characteristics (Byrd, O'Connell, Di Tommaso, & Kelly, 2014). However, spatial heterogeneity of wetland and aquatic vegetation commonly results in mixed pixels, and inundation of wetland vegetation significantly changes the spectral signal, reducing the utility of narrow band indexes such as those centering on the red edge for measuring plant condition (Turpie, 2013). For submerged vegetation, water column optical properties and absorption of near infrared and shortwave infrared radiation also complicate the use of narrow band indexes, particularly those in the infrared regions.

The water column is an effective absorber of near and shortwave infrared energy, whereas terrestrial and vegetated surfaces have relatively high reflectance in these regions. These differences have long been



**Fig. 2.** Representative reflectance spectra of emergent, floating and submerged aquatic vegetation measured above water. The inset graph shows the above water surface reflectance of submerged vegetation under 1 m of water (CHL = 0.8 mg m$^{-3}$, TSM = 0.7 g m$^{-3}$, and CDOM$_{(440)}$ = 0.2 m$^{-1}$).

exploited for detecting surface water extent and inundation using multispectral data (e.g., McFeeters, 1996). However, high spectral resolution is needed to estimate biogeochemical parameters in the water column or the benthos in inland waters (Mouw et al., 2015). In the optically complex waters typically found in freshwater systems there are interacting effects of the absorption and scattering processes on the reflectance spectrum due to the dissolved and suspended organic and inorganic material in the water column and the reflectance of the bottom (in clear or shallow-water systems where photons are not completely attenuated by the water column). High spectral resolution data provides the spectral bands and information redundancy needed for accurate biogeochemical parameter retrievals (Devred et al., 2013) from water bodies that have complex interacting processes influencing the measured spectra. Recommendations have been made recommending optimal band positions to measure water column and benthic properties, however, these vary by environment and by dataset (Lee, Carder, Arnone, & He, 2007; Lee, Shang, Hu, & Zibordi, 2014 and references therein), and none adequately account for inland water quality conditions. High spectral resolution data eliminate the need to select the optimal number of bands and positions, and thus enable retrievals across a wider range of conditions and environments.

The visible and near infrared regions (400–800 nm) are the most relevant regions for measuring the absorption and scattering properties and the suspended and dissolved materials in the water column. However, the longer near and shortwave infrared regions are still important for accurate water column measurements because they are needed for atmospheric correction, which is critical to estimating water quality and plant canopy biochemistry and vegetation species discrimination (Devred et al., 2013; Ustin et al., 2004). For example, water vapor absorbs at 940 nm and 1130 nm, whereas liquid water absorbs at 980 and 1200 nm, which allows for differentiation of different phases of water. High spectral resolution data in the near and shortwave infrared regions may enable accurate estimations of atmospheric water vapor over water bodies (Gao & Goetz, 1990; Gao, Heidebrecht, & Goetz, 1993), however there are still errors associated with simultaneous liquid and water vapor retrievals (Thompson et al., 2015).

When the concentration of chlorophyll-a in the ocean water column increases, the peak in reflectance shifts from blue to green. Thus, blue-green band indexes have successfully been used for decades in ocean color remote sensing to estimate the concentration of CHL (O'Reilly et al., 1998). However, the adaptation of these indexes to turbid freshwater systems is complicated by the influence of dissolved organic matter and suspended particles on the reflectance spectrum. Dissolved organic matter strongly absorbs light in the blue region of the reflectance signal, and suspended matter absorbs and backscatters light, shifting the peak of the reflectance to longer wavelength when there is more scattering and absorbing material in the water column (Dekker & Peters, 1993; Gitelson, 1992; Le et al., 2013). In shallow or relatively clear water where photons are not completely attenuated by the water column, the reflectance properties of the bottom further influence the signal.

Fig. 3 shows five reflectance spectra from four different lakes representative of different water quality conditions, ranging from low to very high CHL concentrations. Reflectance was measured above the water surface with an ASD FieldSpec spectrometer. Table 2 summarizes the characteristics of the lakes and the CHL concentration measured concurrent with the reflectance spectra. Chlorophyll-a has a distinct absorption feature near 660–690 nm, evident in reflectance spectra from the meso- and eutrophic lakes, Lake Idro, Lake Mantua and Lake Trasimeno (Fig. 3). The influence of phycocyanin on absorption at 620 nm can also be seen in these lakes' spectra. High total suspended matter concentration in Lake Trasimeno increases the scattering and thus increases the overall reflectance, as well as creating a reflectance peak in the near-infrared. The spectra in Fig. 4 provide an example of some typical water quality conditions, however, the ranges of freshwater systems vary much more than these examples. For a more complete example of cases, see Dekker et al. (2001).

### 2.4. Spatial resolution

Spatial resolution is one of the primary limiting factors in the application of satellite remote sensing to freshwater ecosystems (Ozesmi & Bauer, 2002). When considering spatial resolution requirements for inland water systems, the determining factor is the pixel size of the sensor system relative to the size of ecosystem of interest. This will vary depending on the type of system, the particular geometry of the feature, and the geography of the target region. We compared the number of resolvable inland and freshwater ecosystems from space using the CORINE Land Cover 2006 v. 16 seamless vector data for Europe (scale ~ 1:100,000; Buttner, Kosztra, Maucha, & Pataki, 2012) and the GEODATA TOPO 250K Series 3 seamless vector data for Australia (scale = 1:250,000; Australia, Geoscience, 2006) as base datasets. We considered a sensor able to effectively measure a water body when the body was four times the size of a pixel to ensure the pixel is "pure" and will not contain any significant signal from spectral mixing with surrounding land or terrestrial vegetation. Thus, in order to resolve a lake at 60 m pixel resolution, 16 (4 × 4) pixels or a 240 m × 240 m area is required to consider the polygon detectable. This is potentially a conservative estimate, but ensures only pure pixels are considered as "observable."

Fig. 4 shows the percent of total freshwater ecosystem polygons detectable from satellite datasets with Landsat-like spatial resolution (30 m), HyspIRI-like spatial resolution (60 m), MERIS-like spatial resolution (250 m) and MODIS-like spatial resolution (1000 m). Based on this analysis, it appears European freshwater ecosystems are more suitable for coarse spatial scale satellite remote sensing measurement. In Europe, nearly all freshwater ecosystems (including ponds, lakes and reservoirs) are observable at both the Landsat and HyspIRI pixel resolutions. The number of resolvable systems does not notably decrease until pixel sizes reach MERIS-like 300 m resolution. However, in Australia there is a notable decrease in the number of polygons detectable when pixel size increases from 30 m to 60 m, and virtually no natural freshwater ecosystems are detectable at MODIS-like resolution.

Given the geomorphology of the two continents, it is unsurprising that there are differences in the observability of freshwater ecosystems. Europe was recently glaciated and has many areas of sharp relief,
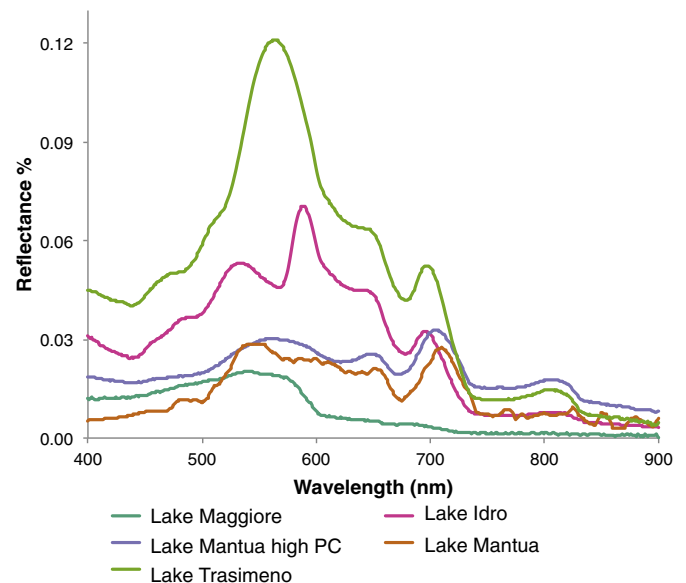
**Fig. 3.** Representative reflectance of five water quality conditions measured in situ with an ASD FieldSpec spectroradiometer in Italian lakes.

**Table 2**
Chlorophyll-a concentration in lakes representing oligotrophic to eutrophic conditions.

| Lake | CHL (mg m$^{-3}$) | Description | Other information |
|---|---|---|---|
| Maggiore | 1.16 | Large deep, peri-alpine oligotrophic | Clear blue lake<br>Secchi depth = 15 m |
| Idro | 16.5 | Large deep, peri-alpine meso-eutrophic | Cyanobacteria bloom CPE = $3.3 \times 10^{-6}$ cells/L |
| Trasimeno | 13.8 | Large, shallow, endorheic meso-eutrophic | Highly turbid, TSM = 30 g m$^{-3}$ |
| Mantua (purple) | 57.5 | Small shallow, fluvial, artificial eutrophic | Cyanobacteria bloom CPC = 31.25 mg m$^{-3}$ |
| Mantua (orange) | 93.8 | Small shallow, fluvial, artificial eutrophic | High concentrations of CHL corresponding to a phytoplankton bloom |

resulting in runoff and drainage patterns that lead to more spatially simple and pseudo-symmetrical polygons. Australia, on the other hand, was largely unglaciated, has much lower relief and exceptionally long hydrologic residence times, resulting in sinuous, spatially complex systems not amenable to observations using large pixels. These estimates of detectable freshwater ecosystems are predicated on the assumption that the base vector datasets are accurate and comparable, which is not entirely met. For example, the base vector layers are of different mapping scales, though on the same order of magnitude. While we consider our estimates to be conservative based on the $4 \times 4$ pixel requirement, they could also potentially be overestimates if the vector layers do not represent small or isolated water bodies and wetlands. However, we can conclude that the suitability of HyspIRI's proposed spatial resolution of 60 m for global freshwater ecosystem measurements will vary geographically based on both the geomorphology of each continent, which will control the size and shape of the freshwater systems.

### 2.5. Temporal resolution

Different freshwater ecosystem processes occur on different temporal scales. Freshwater systems are highly dynamic, and ecosystem function and response is largely driven by hydrology. Inundation period, extent and frequency are some of the primary drivers of aquatic ecosystem variability in primary production, nutrient cycling and other biogeochemical processes both in the water column and for wetlands (Carpenter et al., 2011; Mackay et al., 2012; Stendera et al., 2012). Capturing these dynamic events may be challenging for an optical satellite mission because cloud cover, sun glint, smoke, and occasionally forest cover bias observations, resulting in irregular time series that may obscure important events.
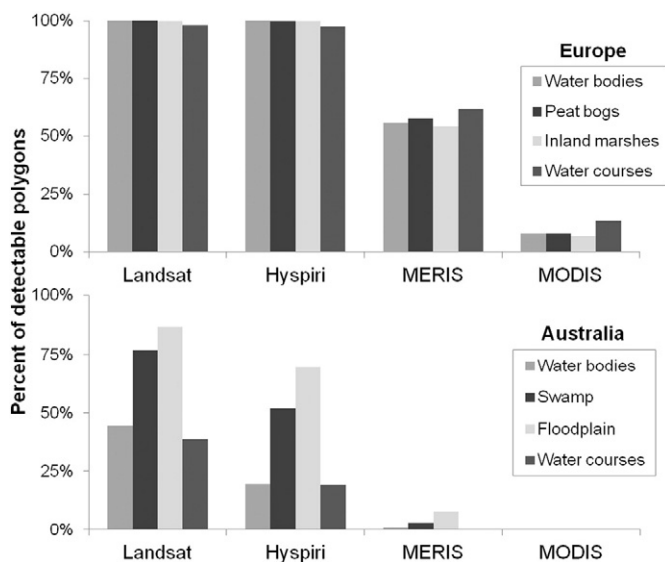


**Fig. 4.** European (top) and Australian (bottom) freshwater systems observable from satellite remote sensing of varying spatial resolutions. The number of freshwater systems on a continent that can be resolved by satellite remote sensing is dependent on the spatial resolution of the sensor, and the size and geometry of the water body.

When considering the temporal resolution of an optical satellite mission, we define two types of temporal resolution, the designed resolution (~19 days at the equator for HyspIRI, shorter at higher latitudes), and the effective resolution, which is determined by the cloudiness and amount of sun glint on the water surface relative to the revisit frequency. Mercury et al. (2012) estimated that HyspIRI's 19 day equatorial revisit cycle (shorter at higher latitudes) will result in 83% cloud free coverage quarterly, and >99% cloud free coverage on an annual basis. Diurnal and daily variations in processes like ecosystem respiration or the development and movement of a harmful algal bloom may not be detectable at this effective resolution. However, HyspIRI's effective resolution is likely suited to measuring seasonal dynamics such as wetland phenologic change (Davranche, Lefebvre, & Poulin, 2010), aquatic invasive species response to management (Santos et al., 2009), or the seasonal phytoplankton community composition of a lake and its detailed bio-optical properties (Devred et al., 2013) because these can be characterized on a quarterly and annual basis.

There are also interactions and tradeoffs between the factors determining the effective temporal resolution. These factors vary geographically and may influence the observability of freshwater ecosystems. While the designed temporal resolution of HyspIRI will provide several day revisit time at high latitudes, the persistent cloud cover common in high latitudes could reduce the effective resolution (Mercury et al., 2012). For instance, even though Fig. 2 suggests that European freshwater ecosystems are more observable than Australian ones based on the spatial resolution of HyspIRI, the higher cloud cover in Europe reduces the effective temporal resolution, and may reduce the overall observability of freshwater ecosystems in Europe. An equatorial mid-morning ascending orbit will increase the likelihood of sun glint at low latitudes, thus decreasing the effective resolution, although the high spectral resolution of HyspIRI could provide the data needed to correct some sun glint if it occurs below sensor saturation levels (Devred et al., 2013; Kutser, Vahtmäe, & Praks, 2009).

Finally, there is strong seasonality in the observability of freshwater ecosystems (Mercury et al., 2012). Thus, in monsoon regions, the precipitation patterns will bias regular observations to dry season conditions. Understanding freshwater ecosystem responses to monsoons and disturbance events such as cyclones may be limited by HyspIRI's effective resolution, and may take more time to assess.

### 2.6. Radiometric capability and its impacts on spatial resolution

The following three instrument characteristics interact affecting the radiometry capability of an aquatic sensor: 1) radiometric resolution, and 2) signal-to-noise ratio (SNR) and 3) radiometric dynamic range. The radiometric resolution of a sensor determines the lowest level of radiance or reflectance that a sensor can reliably detect per spectral band and it depends on the sensor digitization (e.g. 8 vs. 14 bits, Vanhellemont & Ruddick, 2014). The SNR indicates how many times the signal would be larger than the total noise level. For freshwater ecosystems, the sensitivity of the sensor, expressed as SNR, is critical to making accurate biophysical measurements of both the water column and of wetland vegetation where inundation affects the vegetation signal. This is because a sensitive sensor is needed to measure small changes in the low signal of water leaving radiance that is strongly affected by

atmospheric variability, air–water interface reflections and refraction from diffuse and direct sky and sunlight (Brando & Dekker, 2003; Hochberg et al., 2011; Hu et al., 2012; Wettle, Brando, & Dekker, 2004). Another equally important feature of sensor performance for successful measurement of freshwater systems is sufficient dynamic range to be able to make sensitive measurements over low radiance pixels (water) while not saturating over neighboring bright pixels (land or sunglint).

The combined effects of SNR and dynamic range impact the accuracy of biophysical retrieval (e.g., Hu et al., 2012; Vanhellemont & Ruddick, 2014). For example, when Giardino, Brando, Dekker, Strömbeck and Candiani (2007) used Hyperion to measure CHL and TR in Lake Garda in Northern Italy, they had to convolve a $5 \times 5$ low pass filter over the image to reduce the effects of the sensor's poor SNR and environmental noise (Brando & Dekker, 2003; Wettle et al., 2004), effectively reducing the spatial resolution from 30 m to 150 m. Similarly, Vanhellemont and Ruddick (2014) found it necessary to bin Landsat 7 ETM+ data to $9 \times 9$ pixels (270 m) to reach the noise equivalent of Landsat 8 OLI, and had to further bin the data to $11 \times 11$ (330 m) due to the limited digitization (8 bits) of Landsat 7 ETM+. Freshwater ecosystems are spatially complex, and typically have both low (water) and high (land) radiance targets in a single scene, making simultaneous measurement of both problematic. The high SNR and large dynamic range proposed for the HyspIRI mission makes it uniquely well designed for measuring freshwater ecosystems accurately and moderate to high spatial resolution.

### 2.7. Current observation capabilities

For every type of measurement, there are tradeoffs in sensor resolution. Fig. 5 shows some of the most common satellite sensors used for freshwater ecosystem measurements and their relation in terms of spectral (x-axis), temporal (y-axis), and spatial resolution (size of the bubble). HyspIRI's proposed spectral, temporal and spatial characteristics occupy an observation space shared with only a few other satellite missions. However, HyspIRI's observational capabilities make it unique and necessary for freshwater ecosystem measurements, as it occupies a unique niche in sampling space. Freshwater ecosystem measurements from satellite remote sensing can be classified based on the sampling strategy and frequency. We categorize these different schemes into 1) continuous samplers, 2) targeted mappers, and 3) global mappers. Continuous samplers are geostationary satellites that can image high temporal frequency (e.g., Korea's Ocean Color Satellite GOCI that makes a measurement once an hour) of a specific location to provide near-continuous monitoring of dynamic processes such as harmful algal blooms and river plumes. Continuous samplers provide coarse spatial resolution over a specific, targeted region. Targeted mappers can be considered pseudo global mappers. Also in a lower earth orbit (although not necessarily sun synchronous, e.g., the Hyperspectral Imager for the Coastal Ocean, HICO, onboard the International Space Station), targeted mappers acquire data over particular areas based on data acquisition requests (e.g., NASA's EO-1 Hyperion or commercial missions suitable for freshwater like Worldview 2 and 3; WV2, WV3), or regular acquisitions over a region of interest (e.g. the Italian Space Agency's proposed PRISMA mission, or the German Environmental Mapping and Analysis Program) that will provide mapping-like capabilities over a specific region.

Fig. 5 shows the observation capabilities of common current and near to launch sensors in terms of temporal, spectral, and spatial resolutions. Several missions, such as the soon to be launched Sentinel-2 Multispectral Instrument (S2-MSI) provide different spectral bands at different pixel resolutions. Thus, while S2-MSI will have 13 spectral bands across the visible, near and shortwave infrared regions, it will only have four broad "multispectral bands" in the visible and near infrared regions at 10 meter pixel resolution.
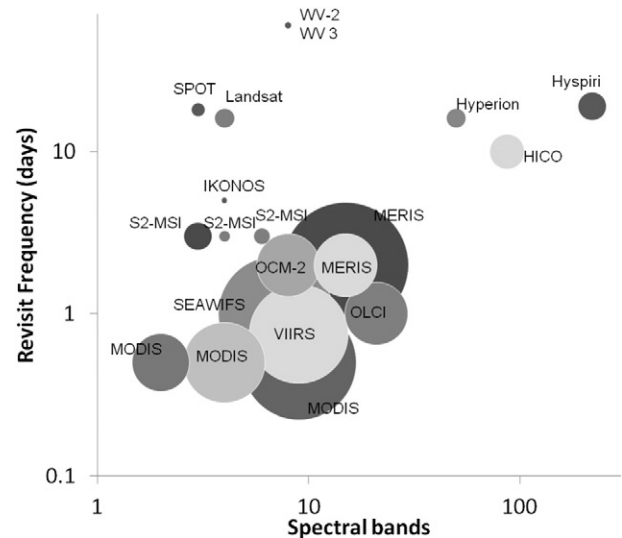


**Fig. 5.** The spectral (x-axis), temporal (y-axis), and spatial (size of the bubble) characteristics of satellite sensors commonly used for freshwater ecosystem measurements. Note: sensors that provide different spatial resolutions are plotted separately, and sensors with overlapping resolution characteristics are slightly jittered for graphing purposes.

Global mappers are valuable for providing regular, repeated measurements of the globe over long periods of time. They typically are also archival missions, meaning they provide a time series of regular observations. Archival global mappers are the most important category of measurement for addressing multiple end user goals of resource monitoring and ecosystem science. Archival global mapping missions with free and open data access policies have transformed scientific understanding of earth surface processes (National Research Council, 2007; Wulder et al., 2012), and provide the most valuable datasets for monitoring (e.g., McCullough, Loftin, & Sader, 2012), and understanding freshwater ecosystem processes and change (e.g., Olmanson, Brezonik, & Bauer, 2014). While Fig. 5 depicts the observation capabilities of common current and near-ready to launch satellite missions, it includes continuous and targeted mappers, such as Worldview 2 & 3 and Hyperion which may not be suited for ecosystem change measurements. Fig. 6 explicitly summarizes the global mapping capability current and near future global mapping capability for freshwater ecosystem science and management. In comparison with current global mapping capabilities, HyspIRI occupies a unique measurement space in both its spatial resolution and temporal resolution, and provides significantly more spectral information than any other global mapper (Fig. 6).

## 3. Case studies

The following case studies illustrate how the characteristics of a hyperspectral global mapping satellite mission, such as the planned HyspIRI mission, address the needs of freshwater aquatic system scientists and managers. We use as our example for freshwater aquatic ecology the remote sensing of primary producers. In the following case studies we highlight published data and existing methods, demonstrating the maturity of the science. However, each case study demonstrates existing gaps in the spatial, temporal, and spectral characteristics of the application, highlighting the need of a mission that will fill these gaps.

### 3.1. Site description

The Mantua lake system is an important freshwater wetland system in Northern Italy that provides critical habitat for aquatic vegetation and water birds in the region. The Mantua system is formed by the damming of the Mincio River, a tributary of the Po, and fed by Lake Garda, the largest lake and longest river of Italy, respectively. The lake waters are
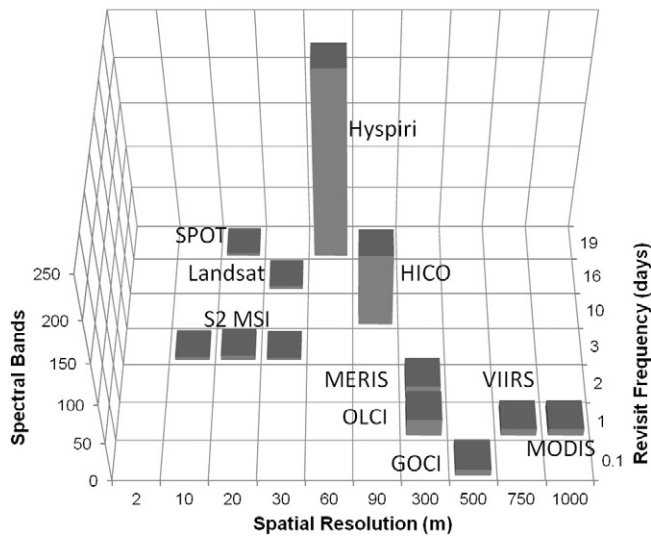
**Fig. 6.** The spectral, spatial and temporal characteristics of current and near future global mappers commonly used for freshwater ecosystem measurements.

productive, characterized by eutrophic to dystrophic levels: chlorophyll concentrations average $32.8 \pm 41.8$ mg m$^{-3}$, and can reach up to 280 mg m$^{-3}$ (see Bolpagni et al., 2014 and references therein). The phytoplankton communities in the Mantua lake system are typical of eutrophic and hypertrophic systems rich in organic matter: diatoms in the spring and cyanophytes and chlorophytes in the summer (Pinardi, Bartoli, Longhi, & Viaroli, 2011). From spring to autumn, a large part of the surface of the lakes is covered by dense stands of floating emergent macrophytes, including the exotic invasive lotus flower (*N. nucifera*), as well as common water chestnut (*T. natans*), spatterdock (*Nuphar lutea*) and water lily (*Nimphaea alba*).

Recent studies (e.g., Bolpagni et al., 2014; Bresciani, Giardino, et al., 2009; Bresciani et al., 2013; Villa, Bresciani, Braga & Bolpagni, 2014; Villa, Mousivand & Bresciani, 2014) have shown the capability of three sensors mounted on ground, airborne and satellite platforms, in observing optical properties of different primary producers of these lakes. In this section we summarize their findings and address how a hyperspectral global mapping mission could provide deeper knowledge on the aquatic ecology of the Mantua lake system.

*3.2. Cyanobacteria blooms*

Cyanobacterial blooms can lead to hypoxia and alter food-web dynamics (Anderson, Glibert, & Burkholder, 2002), and may pose a substantial health risk for communities accessing affected water for drinking, irrigation and recreation if the blooms contains toxins. If a cyanobacteria bloom is toxic, it can affect liver cells and respiratory health (Codd, Lindsay, Young, Morrison, & Metcalf, 2005), and long term exposure may lead to neurodegenerative diseases and Alzheimer's-like dementia (Dunlop, Cox, Banack, & Rodgers, 2013). Phycocyanin (PC), the diagnostic pigment for cyanobacteria detection, is detectable using optical remote sensing (Dekker, Malthus, & Goddijn, 1992; Dekker, Malthus, Wijen, & Seyhan, 1992; Simis, Peters, & Gons, 2005) due to PC spectral absorption near 620–630 nm. This narrow PC absorption feature can be discriminated from CHL, which has an absorption a feature independent of PC around 676 nm (Kutser, 2009).

We measured the cyanobacteria trend in the Mantua lakes using in situ data gathered from an optical system designed for high temporal frequency acquisition of high spectral resolution radiometric measurements. The optical system is called the multiplexer radiometer irradiometer (MRI), and is based on a commercial optical multiplexer described in (Bresciani et al., 2013). The MRI was deployed on a pontoon in the upper basin of the Mantua lakes from 2 September to 2

October 2011. The PC index was calculated using the algorithm of Kutser et al. (2006) (Eq. 1):

$$PC = \frac{\rho_{max(640-650)}}{\rho_{min(610-630)}}, \qquad (1)$$

where the PC index is the simple ratio of maximum reflectance between 640 and 650 nm and the minimum reflectance between 610 and 630 nm. The results are shown in Fig. 7.

Fig. 7 shows the daytime and day-to-day dynamics of cyanobacteria (mainly composed of *Planktolyngbya limnetica* and *Cylindrosperopsis raciborskii*) in Lake Mantua from a point based measurement. Similar to Gons, Hakvoort, Peters, and Simis (2005), the index makes use of narrow bands at the key spectral features of phycocyanin. High spectral resolution is necessary for detecting PC spectral features, especially because the location of the spectral features varies based on the relative concentration of PC to CHL (Gitelson, Schalles, & Hladik, 2007). Of the legacy and near-future spaceborne multispectral sensors, only MERIS and OLCI have the spectral bands in the positions required to detect PC (Kutser, 2009), and even this sensor lacks the high spectral resolution to detect PC when it is present in large quantities (Kutser et al., 2006).

Fig. 7 also shows the daytime variation in PC and the value of PC measured at 10:30 am, the approximate schedule for a mid morning satellite overpass. From these results, it is clear that a mid morning overpass would adequately represent the daily median PC of Lake Mantua. Some species of cyanobacteria can regulate their buoyancy, forming non uniform distributions through the water column (Paerl, 2008; Reynolds, Oliver, & Walsby, 1987). When coupled with advective currents, the spatial distribution of a cyanobacterial bloom can be patchy, making it difficult to monitor from fixed depth or point based sampling stations (Hunter, Tyler, Willby, & Gilvear, 2008; Kutser et al., 2006). It is unclear whether the daily trend, notably the two peaks in PC in mid and late September followed by the PC decrease in October is due to changing bloom conditions, or patchiness from vertical and horizontal movement of the PC. The temporal frequency of a global mapping mission with a revisit time similar to Landsat fails to provide adequate coverage
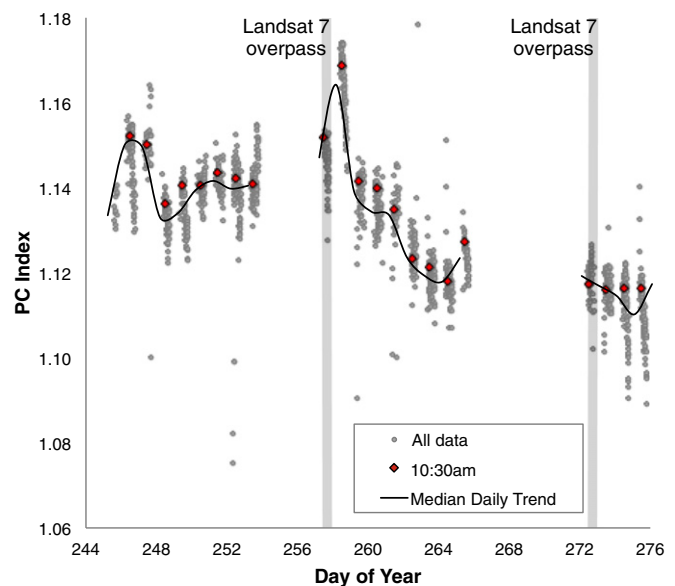


**Fig. 7.** Phycocyanin (PC) index in Upper Mantua Lake, calculated from an above-water in situ high temporal frequency, high spectral resolution radiometer using the algorithm of Kutser et al. (2006). The measurements are plotted in gray dots, the measurement made at 10:30 am is plotted in red, and the black line indicates the spline-smoothed daily median trend. The gray vertical bars indicate the overpass dates of Landsat 7.

of the temporal dynamics evident in this example (Fig. 7). High temporal resolution imaging spectroradiometry from geostationary satellite platforms could synoptically capture the temporal dynamics of cyanobacterial blooms. However, spatial and spectral resolutions may limit the practical application of such platforms for systems such as the Mantua lakes.

### 3.3. Aquatic vegetation phenology

In addition to providing valuable habitat to multiple freshwater ecosystem species, emergent wetland vegetation have high rates of net primary production and evapotranspiration, drive a large portion of wetland carbon formation and storage, and play an important role in wetland sediment stability and accretion (Byrd et al., 2014; Zhou & Zhou, 2009). Indeed, the emergent common reed Phragmites may be the most widely globally distributed wetland species (Zhou & Zhou, 2009). Floating and submerged plants provide important structuring for freshwater ecosystems, influencing the physical and chemical environment and food web (Liu, Zhang, Yin, Wang, & Qin, 2013; Meerhoff, Mazzeo, Moss, & Rodríguez-Gallego, 2003; Santos, Anderson, & Ustin, 2011; Vanderstukken, Declerck, Decaestecker, & Muylaert, 2014). Understanding the growth and distribution of aquatic vegetation is useful in understanding subsequent ecosystem properties. Remote sensing is powerful and effective to monitor vegetation status, growth and biophysical parameters, providing a synoptic assessment and permitting retrospective change detection analyses in a cost effective way (Coppin & Bauer, 1994; Munyati, 2000). Most of the methods adopted to study vegetation from satellite observations have been based on vegetation indexes (VIs), that have demonstrated enormous usefulness as indicators of green terrestrial vegetation growth and vigor (Wickland, 1989). For aquatic vegetation, VIs have been used for mapping and monitoring common reed vegetation (Davranche et al., 2010; Khanna et al., 2011; Poulin, Davranche, & Lefebvre, 2010; Villa, Laini, Bresciani, & Bolpagni, 2013), assessing vegetation health (Bresciani, Bolpagni, Braga, Oggioni, & Giardino, 2012; Bresciani, Stroppiana, Fila, Montagna & Giardino, 2009), estimating leaf area index (Zhou & Zhou, 2009), and for revealing the presence of phenomena such as the die-back syndrome of common reed aquatic vegetation (Davranche et al., 2010; Evans, Lyons, Barber, Stone, & Hardy, 2011).

We used the recently developed Water Adjusted Vegetation Index (WAVI; Eq. 2), which has been proven to be a diagnostic index for detecting a variety of macrophyte types (Villa, Brescianiet al., 2014; Villa, Mousivand et al., 2014), to capture the main types of aquatic vegetation growing in the Mantua lakes. The WAVI is given by the following:

$$(1+L)\frac{\rho_{NIR}-\rho_{BLUE}}{\rho_{NIR}+\rho_{BLUE+L}},\qquad(2)$$

where L is a background signal correction factor (Villa, Mousivand et al., 2014) (set to 0.5 for this case study), $\rho_{NIR}$ is the measured reflectance in a selected near infrared band (850–880 nm for this case study), and $\rho_{BLUE}$ is the measured reflectance in a selected blue band (450–510 nm for this case study).

The index was applied to 14 Landsat-8 OLI (L8) scenes acquired from April to November 2013, which have been corrected for atmospheric effect with ATCOR (Richter & Schläpfer, 2011). The WAVI was then derived from normalized difference response of blue (L8 band 2) and near-infrared (L8 band 5) spectral ranges, adjusted for water background effect. Based on a vegetation survey performed during 2013 over Mantua lakes system we defined vector polygons of homogeneous macrophytes stands covered by monospecific stands or a mixture of two species: 1) monospecific emergent helophytes (P. australis), 2) monospecific emergent rhyzophytes (N. nucifera), 3) small and dense free-floating plants (mixture of Salvinia natans, Spirodela polyrrhiza), and 4) composite association of floating leaved vegetation (mixture of T. natans, N. alba), 5) dense submerged vegetation (C. demersum at

~5 cm depth), 6) Open water where no vegetation was identified. All polygons representing each macrophyte stand over the study area were used to extract the WAVI values for each date in L8 time series.

Fig. 8 shows the multi-temporal WAVI profiles presented as average and standard deviation describing seasonal variation in phenology from Spring to Autumn for different aquatic vegetation communities. Emergent helophytes (P. australis) and rhyzophytes (N. nucifera) show a rapid rise in the calculated WAVI, indicative of an increase in biomass and green leaves. Small dense free floating (S. natans + S. polyrrhiza) and floating leaved (T. natans + N. alba), communities expand their cover over the water surface later in the season and show higher variability due to the assemblage heterogeneity. The seasonal variation in the WAVI calculated for submerged vegetation (C. demersum) is likely influenced by changing water level over the season. The WAVI profile for water is stable across the year and lower than all the aquatic vegetation communities.

The broad bands and the 16-day repetition cycle of Landsat 8 allowed us to capture the whole aquatic vegetation heterogeneity present in Mantua lake system area and to assess their specific phenological cycle. This example shows that in a temperate freshwater ecosystem that has clear cloud free conditions during the growing season, the effective resolution is suited to observing phenology. While in this example the target macrophyte communities were identified based on field data, hyperspectral imagery would allow the identification and mapping of each community based on their spectral properties. Hence the HyspIRI proposed temporal and spectral resolutions would enable this phenological analysis with a lesser need for dedicated field surveys. These combined resolutions would also permit to identify other processes of interest such as leaf biochemistry, functional type, and understanding invasion strategies and dynamics.

### 3.4. Chlorophyll-a concentration

Providing a proxy of phytoplankton biomass and being an indicator for eutrophication and primary production, CHL concentration is an important parameter in water's ecology and management. Since the last century satellite remote sensing has been successfully used to map the spatial pattern of CHL in lakes (e.g., Lindell, Pierson, Premazzi, & Zilioli, 1999). To the aim, various methods were developed, both based on bio-optical modeling (e.g., Pierson & Strömbeck, 2001), and on semi-analytical methods based on band ratios at wavelengths with unique CHL absorption features (e.g., Gitelson et al., 2008, Fig. 4).

We estimated the CHL concentration in Mantua lakes using airborne data gathered from APEX (Airborne Prism EXperiment). APEX is an imaging spectrometer that records the electromagnetic radiation in 98 bands between 426 and 910 nm (Itten et al., 2008). The image was acquired on the Upper Lake on 21 September 2011, with a ground resolution of 4 m. The ratio between the average of the APEX atmospherically corrected reflectance measured between bands 690–697 nm and the average reflectance measured at 670–673 nm was converted into CHL concentration according conversion factors specific for Mantua lakes (Bresciani et al., 2013). As shown in Bolpagni et al. (2014), the mean CHL concentration obtained from APEX (16.2 ± 12.5 mg m$^{-3}$) was similar to the mean CHL concentrations measured in situ (15.9 ± 10.6 mg m$^{-3}$).

Fig. 9 shows the map of CHL concentration derived from the APEX image. To exemplify the effect of spatial resolution on observability of water column drivers of primary productivity in Lake Mantua, we convolved the APEX-derived map to the spatial resolution of Landsat, HyspIRI, MERIS and MODIS using nearest-neighbor re-sampling. The maps show how the spatial resize affects the ability to measure the patchy spatial distribution of CHL captured in the 4 m pixel of APEX; the 30 m and the 60 m resolution of Landsat and HyspIRI still allow the spatial trends of CHL concentration to be captured, although finer scale patterns vanish. MODIS does not have the appropriate spatial resolution to assess CHL in the Mantua lakes.
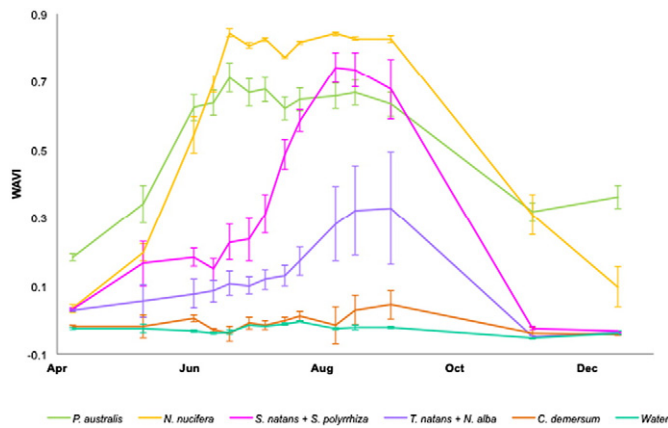
**Fig. 8.** Seasonal variation in WAVI (averages and standard deviations) from Landsat 8 OLI for 5 different aquatic vegetation communities and open water.

Based on our estimates of freshwater ecosystem observability in Section 2.4 (Fig. 4), Lake Mantua is not observable by either MODIS or MERIS, because there is not a 4 × 4 block of pixels contained within the boundary of the water body (Fig. 9). This case study of Lake Mantua illustrates how the often sinuous, riverine shape and spatial complexity

of freshwater systems influence their observability. While there are MERIS pixels present within the water body in Fig. 9, a close comparison of the edges of the water body as resolved by APEX show that the MERIS pixels are mixed with adjacent land and wetland complex pixels. The large levee bisecting the upper northeast portion of lake and the wetland stream complex in the southwest portion of the lake are not resolved at all by MERIS. At the MODIS pixel resolution, there are no pixels that do not contain significant portions of land.

Recently it was suggested that while large spatial resolution sensors such as MODIS and MERIS could not effectively view the majority of freshwater systems, they could be used to measure a selection of water bodies representative of a target ecosystem, serving as "virtual stations" for ecosystem measurement (Dekker & Hestir, 2012). These results challenge that suggestion because a lake that is only resolved by a few large pixels results in a "smoothing" of the CHL measurements; local areas of high concentration are mixed with areas of lower concentration to produce results that maybe indicative of the "average" surface concentration, but may not be informative to interpreting spatial patterns in the data. For example, the large pixels representing "average" surface concentration conditions could impede algal bloom detection, and may obfuscate sources of eutrophication and processes of primary production. In such an instance, using MERIS measurements as virtual stations for ecological understanding of Lake Mantua may be too limited.
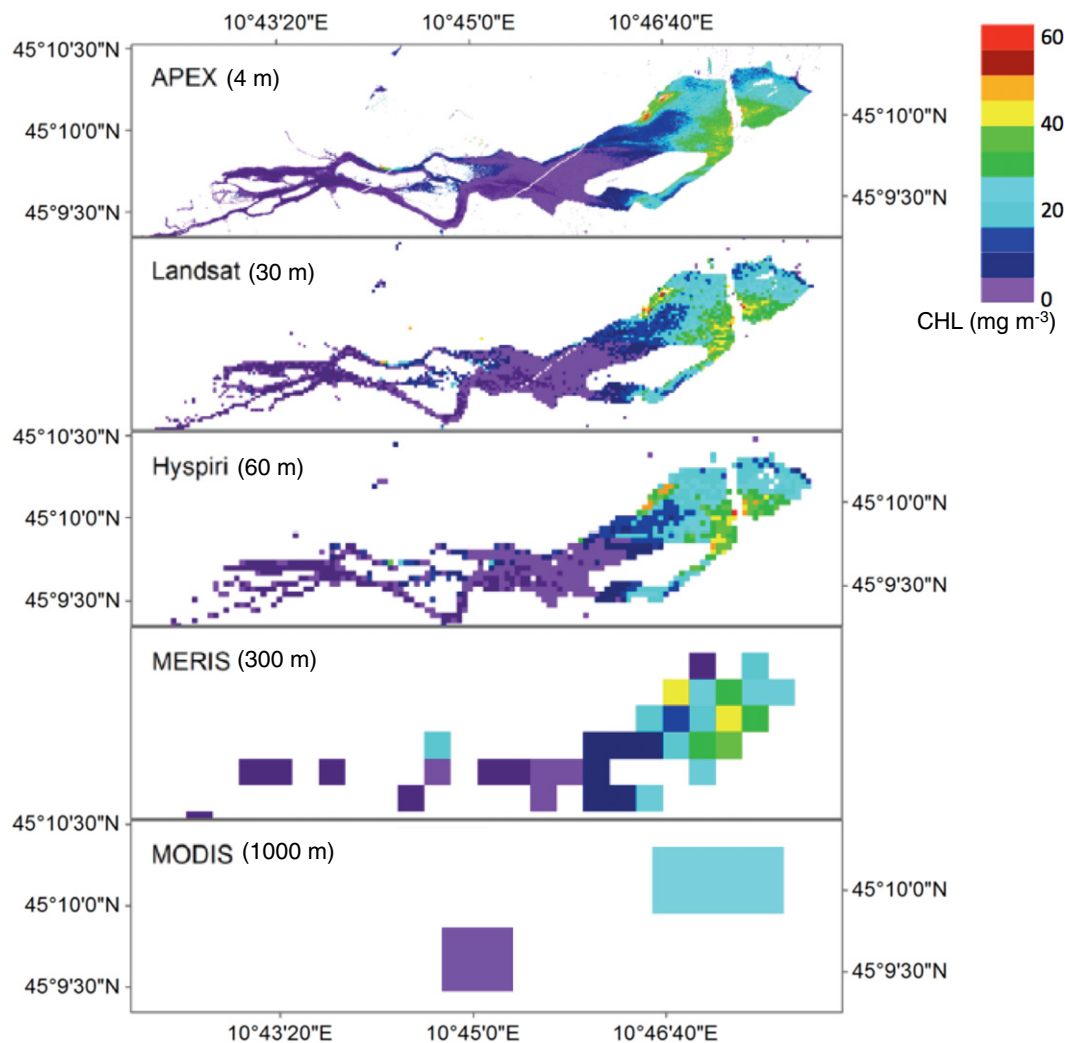


**Fig. 9.** CHL concentration in Upper Mantua Lake from the APEX airborne imaging spectrometer (top), and re-sampled to different sensor spatial resolutions. Color scale ranges from purple to red for CHL ranging from 0 to 60 mg m$^{-3}$.

## 4. Discussion

### 4.1. High spectral resolution data provide advantages

Using existing, published techniques, these case studies demonstrate that a hyperspectral global mapping mission such as HyspIRI meets the measurement requirements of multiple end users for freshwater ecosystem science and management. These case studies, in addition to the robust and increasing literature (Fig. 1) also demonstrate that algorithms for retrieving some freshwater ecosystem biophysical variables are mature. Archival, global mapping missions with multispectral (e.g., Landsat) or narrow band moderate spectral resolution sensors (e.g., MERIS) have provided high quality data from which many ecosystem process studies of the terrestrial and coastal zone have been achieved. However, these sensors have measurement resolution tradeoffs that make them unsuited for freshwater ecosystem studies. For example, while Landsat has the spatial resolution for freshwater systems, it cannot provide the spectral resolution to resolve individual phytoplankton pigments. Similarly, MERIS spectral bands are well suited for water column characterization and high frequency measurements, but the pixel size limits the number of freshwater systems resolvable from that sensor.

Using spectral indices in a semi-empirical approach provides easily calculable estimates of water column and plant canopy properties (e.g. Kutser et al., 2006; Davranche et al., 2010; Bresciani et al., 2013; Villa, Bresciani et al., 2014). Narrow band indices enabled by hyperspectral data that highlight specific absorption features can also be used to select and empirically calibrate or modify broad band indices, providing a link between hyperspectral and multispectral datasets (Das & Seshasai, 2014). However, such approaches require different relationships for each property of interest, and the underlying empirical relationships may not be extensible to new locations or times. On the other hand, radiative transfer inversion of remote sensing spectra can simultaneously estimate water column properties such as CHL, PC, CDOM, non-algal particulate matter and water depth, and plant canopy properties such as leaf pigment, canopy water content, canopy dry matter and leaf area index. Hyperspectral data leads to more successful inversion of a larger number of properties and creates the potential for measuring new properties (e.g., phytoplankton functional types, particulate carbon) because the additional information helps to overcome the underdetermined problem (Devred et al., 2013).

Unlike multispectral terrestrial and ocean color missions that have band positions selected for targeted applications that necessarily limit the biophysical variables retrieved from a given sensor, a hyperspectral mission (with necessarily high fidelity) provides the spectral information needed to retrieve multiple biophysical variables simultaneously from both the water column and wetland/riparian components of freshwater ecosystems. The result of this capability is that by using just one measurement, it is possible to gain improved understanding of ecosystem properties and processes. In our case studies, we presented the estimation of only a single biophysical variable at a time. While current algorithms tend to be targeted to retrieve just one or a few biophysical variables at a time (e.g. Kutser et al., 2006; Bresciani et al., 2013; Villa, Bresciani et al., 2014), algorithm developments supported by comprehensive high quality hyperspectral datasets may lead to algorithms that perform multiple variable retrievals from a single processing chain. A hyperspectral global mapping mission will provide the data needed to investigate robust algorithm development, including a global atmospheric correction solution and new biophysical variable retrievals, such as phytoplankton functional types (Devred et al., 2013).

### 4.2. Global mapping, archival missions and access are keys to end user uptake

Of the three sampling schemes provided by satellite remote sensing missions, global mapping missions may be arguably the most important

for whole of ecosystem studies because they make systematic, repeated measurements, providing both a global picture with synoptic regional sampling and local detail. This is particularly important for freshwater ecosystems, where some of the largest drivers of biodiversity require repeated synoptic observations. These drivers include land use and land cover change and eutrophication, watershed deforestation, habitat connectivity (both longitudinal and latitudinal flow connectivity), and hydro-period (Stendera et al., 2012).

Archival global mapping missions are critical to end user uptake because they provide measurements all over the world. Open access and free data policies enable wider use and broader management and scientific uptake. Operational algorithms implemented in open source software platforms (e.g., SeaDAS and BEAM) provide tools that lower the "hyperspectral" entrance barrier and allows more diverse earth science applications. This is especially critical for freshwater ecosystem science and management in developing nations and regions with poor infrastructure and limited access to traditional sampling technologies. One of the greatest end-user needs for freshwater ecosystem management is reliable, repeatable inexpensive monitoring (Bresciani et al., 2011), which is in part provided by archival global mapping missions with open access and free data policies. Such missions also serve to meet one of the greatest scientific end-user objectives: ecosystem change detection. Retrospective time series analysis of ecosystem response to land management and climate change and variability is only possible with archival missions.

### 4.3. Observation systems for whole of system characterization

While there are strong arguments to be made for archival global mapping missions, not all freshwater ecosystem characteristics will be observable from such sampling schemes. Clearly, our PC case study demonstrates that a global mapping mission, even with a daily revisit cycle, will not adequately resolve all important ecosystem processes (Fig. 9). While a hyperspectral archival global mapping mission, like HyspIRI, meets a critical gap in our global mapping capabilities (Fig. 8), it also has limitations. The temporal resolution of HyspIRI limits the utility of such a mission to characterize processes such as the development of a harmful algal bloom, and the proposed late-morning ascending equatorial crossing of the satellite may result in substantial amounts of sun glint at low latitudes (Devred et al., 2013), which could result in a loss of valid observations, but could also be used to better characterize wetland inundation (Vanderbilt, Khanna, & Ustin, 2007). Similarly, the spatial resolution of HyspIRI may not be appropriate for all global freshwater ecosystems: while HyspIRI's spatial resolution is more than suitable for more than 90% of Europe's freshwater ecosystems, only 52% of Australia's swamps, and less than 20% of Australia's water courses and water bodies may be detectable at 60 m pixel resolution.

These shortcomings are not surprising: one mission will not solve all observation needs. Optimal freshwater ecosystem sampling schemes should include complementary in situ and satellite observations, including combined optical and radar approaches (Prigent, Matthews, Aires, & Rossow, 2001). Data fusion techniques are mature, allowing researchers to combine spatial and spectral information from one or multiple remote sensing observations or a time series of observations (Bioucas-Dias et al., 2013). Hyperspectral data facilitate bridging the scaling gap from molecular-to ecosystem-to-biome by providing the spectroscopic information needed to resolve and couple radiative transfer models and scale process based models (Schaepman et al., 2009).

## 5. Summary & conclusions

1. Freshwater ecosystems are important societal and ecological resources under threat due to anthropogenic and climate change. Observing freshwater ecosystems from space is challenging because many are relatively small, spatially complex, temporally dynamic,

and optically complex both in the plant canopy and water column. Current sensors cannot meet all of these challenges.

2. The HysplRI mission occupies a unique niche in observational capability in terms of its spectral, spatial, temporal, and radiometric resolution. The resolution characteristics of the HysplRI mission make well suited to observing freshwater ecosystems.

3. HysplRI's high spectral and radiometric resolution enables accurate, simultaneous measurement of riparian, wetland and aquatic plant canopy properties and water column biophysical properties, providing synoptic, whole-ecosystem measurements for understanding ecosystem function and change.

4. We estimate that HysplRI's spatial and effective temporal resolution will detect a large portion of freshwater ecosystem properties at a seasonal time scale. This will provide measurements of plant phenology, but may not capture highly dynamic processes such as potentially harmful algal blooms. Further, the observability of freshwater ecosystems will vary geographically, based on cloud cover and the geomorphology of the landscape, which influences the size, shape, and distribution of freshwater ecosystems.

5. The archival, global mapping mission planned by HysplRI is needed to provide reliable, repeatable monitoring for ecosystem studies and to meet the data requirements of end-users. Open access and free data policies, operational algorithms and open source platforms are needed to lower the hyperspectral entrance barrier for end-users.

## Acknowledgments

## References

Adam, E., Mutanga, O., & Rugege, D. (2010). Multispectral and hyperspectral remote sensing for identification and mapping of wetland vegetation: A review. *Wetlands Ecology and Management, 18*, 281–296.

Alsdorf, D., Melack, J., Dunne, T., Mertes, L., Hess, L., & Smith, L. (2000). Interferometric radar measurements of water level changes on the Amazon flood plain. *Nature, 404*, 174–177.

Amarnath, G. (2014). An algorithm for rapid flood inundation mapping from optical data using a reflectance differencing technique. *Journal of Flood Risk Management, 7*, 239–250.

Ampe, E., Hestir, E., Bresciani, M., Savadore, E., Brando, V., Dekker, A., et al. (2014). A wavelet approach for estimating chlorophyll-a from inland waters with reflectance spectroscopy. *IEEE Geoscience and Remote Sensing Letters, 11*, 89–93.

Anderson, D., Glibert, P., & Burkholder, J. (2002). Harmful algal blooms and eutrophication: Nutrient sources, composition, and consequences. *Estuaries, 25*, 704–726.

Andrew, M.E., & Ustin, S.L. (2009). Effects of microtopography and hydrology on phenology of an invasive herb. *Ecography, 32*, 860–870.

Artigas, F., & Yang, J. (2007). Hyperspectral remote sensing of marsh species and plant vigour gradient in the New Jersey Meadowlands. *International Journal of Remote Sensing, 26*, 5209–5220.

Australia, Geoscience (2006). *GEODATA TOPO 250K Series, 3*, Canberra: Geoscience Australia.

Aylward, Bruce, et al. (2005). *Freshwater ecosystem services. Ecosystems and human well-being: Policy responses, 3.* (pp. 213–256), 213–256.

Becker, B., Lusch, D., & Qi, J. (2007). A classification-based assessment of the optimal spectral and spatial resolutions for Great Lakes coastal wetland imagery. *Remote Sensing of Environment, 108*, 111–120.

Bioucas-Dias, J., Plaza, A., Camps-Valls, G., Scheunders, P., Nasrabadi, N., & Chanussot, J. (2013). Hyperspectral remote sensing data analysis and future challenges. *IEEE Geoscience and Remote Sensing Magazine, 1*, 6–36.

Bjerklie, D., Lawrence Dingman, S., Vorosmarty, C., Bolster, C., & Congalton, R. (2003). Evaluating the potential for measuring river discharge from space. *Journal of Hydrology, 278*, 17–38.

Blondeau-Patissier, D., Gower, J., Dekker, A., Phinn, S., & Brando, V. (2014). A review of ocean color remote sensing methods and statistical techniques for the detection, mapping and analysis of phytoplankton blooms in coastal and open oceans. *Progress in Oceanography, 123*, 123–144.

Bolpagni, R., Bresciani, M., Laini, A., Pinardi, M., Matta, E., Ampe, E., et al. (2014). Remote sensing of phytoplankton–macrophyte coexistence in shallow hypereutrophic fluvial lakes. *Hydrobiologia, 737*, 67–76.

Bowers, D., & Binding, C. (2006). The optical properties of mineral suspended particles: A review and synthesis. *Estuarine, Coastal and Shelf Science, 67*, 219–230.

Brando, V., & Dekker, A. (2003). Satellite hyperspectral remote sensing for estimating estuarine and coastal water quality. *IEEE Transactions on Geoscience and Remote Sensing, 41*, 1378–1387.

Bresciani, M., Bolpagni, R., Braga, F., Oggioni, A., & Giardino, C. (2012). Retrospective assessment of macrophytic communities in southern Lake Garda (Italy) from in situ and MIVIS (Multispectral Infrared and Visible Imaging Spectrometer) data. *Journal of Limnology, 71*, 180–190.

Bresciani, M., Giardino, C., Longhi, D., Pinardi, M., Bartoli, M., & Vascellari, M. (2009). Imaging spectrometry of productive inland waters. Application to the lakes of Mantua. *Italian Journal of Remote SensingRivista Italiana di Telerilevamento, 41*, 147–156.

Bresciani, M., Rossini, M., Morabito, G., Matta, E., Pinardi, M., Cogliati, S., et al. (2013). Analysis of within- and between-day chlorophyll-a dynamics in Mantua Superior Lake, with a continuous spectroradiometric measurement. *Marine and Freshwater Research, 64*, 303–316.

Bresciani, M., Stroppiana, D., Fila, G., Montagna, M., & Giardino, C. (2009). Monitoring reed vegetation in environmentally sensitive areas in Italy. *European Journal of Remote Sensing, 41*, 125–137.

Bresciani, M., Stroppiana, D., Odermatt, D., Morabito, G., & Giardino, C. (2011). Assessing remotely sensed chlorophyll-a for the implementation of the Water Framework Directive in European perialpine lakes. *Science of the Total Environment, 409*, 3083–3091.

Bridgham, S., Moore, T., Richardson, C., & Roulet, N. (2014). Errors in greenhouse forcing and soil carbon sequestration: A comment on Mitsch et al. (2013). *Landscape Ecology, 29*, 1481–1485.

Brodie, J., Schroeder, T., Rohde, K., Faithful, J., Masters, B., Dekker, A., et al. (2010). Dispersal of suspended sediments and nutrients in the Great Barrier Reef lagoon during river-discharge events: Conclusions from satellite remote sensing and concurrent flood-plume sampling. *Marine and Freshwater Research, 61*, 651–664.

Buttner, G., Kosztra, B., Maucha, G., & Pataki, R. (2012). *Implementation and achievements of CLC2006.* Barcelona: European Environment Agency, 65.

Byrd, K.B., O'Connell, J.L., Di Tommaso, S., & Kelly, M. (2014). Evaluation of sensor types and environmental controls on mapping biomass of coastal marsh emergent vegetation. *Remote Sensing of Environment, 149*, 166–180.

Carbonneau, P., & Piegay, H. (2012). *Fluvial remote sensing for science and management.* West-Sussex: Wiley-Blackwell (435 pp.).

Carlson, K., Asner, G., Hughes, R., Ostertag, R., & Martin, R. (2007). Hyperspectral remote sensing of canopy biodiversity in Hawaiian lowland rainforests. *Ecosystems, 10*, 536–549.

Carpenter, D., & Carpenter, S. (1983). Modeling inland water quality using Landsat data. *Remote Sensing of Environment, 13*, 345–352.

Carpenter, S., Stanley, E., & Vander Zanden, M. (2011). State of the world's freshwater ecosystems: Physical, chemical, and biological changes. *Annual Review of Environment and Resources, 36*, 75–99.

Codd, G., Lindsay, J., Young, F., Morrison, L., & Metcalf, J. (2005). Harmful cyanobacteria. In J. Huisman, H.P. Matthijs, & P. Visser (Eds.), *Harmful cyanobacteria* (pp. 1–23). Netherlands: Springer.

Cohen, W., & Goward, S. (2004). Landsat's role in ecological applications of remote sensing. *BioScience, 54*, 535–545.

Coppin, P., & Bauer, M. (1994). Processing of multitemporal Landsat TM imagery to optimize extraction of forest cover change features. *IEEE Transactions on Geoscience and Remote Sensing, 32*, 918–927.

Crétaux, J., Jelinski, W., Calmant, S., Kouraev, A., Vuglinski, V., et al. (2011). SOLS: A lake database to monitor in the near real time water level and storage variations from remote sensing data. *Advances in Space Research, 47*, 1497–1507.

Das, P., & Seshasai, M. (2014). Multispectral sensor spectral resolution simulations for generation of hyperspectral vegetation indices from Hyperion data. *Geocarto International*http://dx.doi.org/10.1080/10106049.2014.9733065.

Davranche, A., Lefebvre, G., & Poulin, B. (2010). Wetland monitoring using classification trees and SPOT-5 seasonal time series. *Remote Sensing of Environment, 114*, 552–562.

Dekker, A., Brando, V., Anstee, J., Pinnel, N., Kutser, T., Hoogenboom, E., et al. (2001). Imaging spectrometry of water. Imaging spectrometry. In F. Meer, & S. Jong (Eds.), *Imaging spectrometry* (pp. 307–359). Netherlands: Springer Netherlands.

Dekker, A., & Hestir, E. (2012). *Evaluating the feasibility of systematic inland water quality monitoring with satellite remote sensing.* Canberra: Commonwealth Scientific and Industrial Research Organization, 123.

Dekker, A., Malthus, T., & Goddijn, L. (1992). Monitoring cyanobacteria in eutrophic waters using airborne imaging spectroscopy and multispectral remote sensing systems. *Proceedings of 6th Australasian Remote Sensing Conference* (pp. 204–214). Wellington: Australasian Remote Sensing and Photogrammetry Association.

Dekker, A., Malthus, T., Wijen, M., & Seyhan, E. (1992). The effect of spectral bandwidth and positioning on the spectral signature analysis of inland waters. *Remote Sensing of Environment, 41,* 211–225.

Dekker, A., & Peters, S. (1993). The use of the thematic mapper for the analysis of eutrophic lakes: A case study in The Netherlands. *International Journal of Remote Sensing, 14,* 799–822.

Del Castillo, C., & Miller, R. (2008). On the use of ocean color remote sensing to measure the transport of dissolved organic carbon by the Mississippi River plume. *Remote Sensing of Environment, 112,* 836–844.

Dennison, P., & Roberts, D. (2003). The effects of vegetation phenology on endmember selection and species mapping in southern California chaparral. *Remote Sensing of Environment, 87,* 295–309.

Devred, E., Turpie, K., Moses, W., Klemas, V., Moisan, T., Babin, M., et al. (2013). Future retrievals of water column bio-optical properties using the hyperspectral infrared imager (HyspIRI). *Remote Sensing, 5,* 6812–6837.

Downing, J., Prairie, Y., Cole, J., Duarte, C., Tranvik, L., Striegl, R., et al. (2006). The global abundance and size distribution of lakes, ponds and impoundments. *Limnology and Oceanography, 5,* 2388–2397.

Doxoran, D., Froidefond, J., Lavender, S., & Castaing, P. (2002). Spectral signature of highly turbid waters: Application with SPOT data to quantify suspended particulate matter concentrations. *Remote Sensing of Environment, 18,* 149–161.

Dronova, I., Gong, P., Clinton, N., Wang, L., Fu, W., Qi, S., et al. (2012). Landscape analysis of wetland plant functional types: The effects of image segmentation scale, vegetation classes and classification methods. *Remote Sensing of Environment, 127,* 357–369.

Dronova, I., Gong, P., & Wang, L. (2011). Object-based analysis and change detection of major wetland cover types and their classification uncertainty during the low water period at Poyang Lake, China. *Remote Sensing of Environment, 115,* 3220–3236.

Dudgeon, D., Arthington, A., Gessner, M., Kawabata, Z. -I., Knowler, D., Lévêque, C., et al. (2006). Freshwater biodiversity: Importance, threats, status and conservation challenges. *Biological Reviews, 81,* 163–182.

Dunlop, R., Cox, P., Banack, S., & Rodgers, K. (2013). The non-protein amino acid BMAA is misincorporated into human proteins in place of L-serine causing protein misfolding and aggregation. *PLoS ONE, 8,* e75376.

Evans, B., Lyons, T., Barber, P., Stone, C., & Hardy, G. (2011). Dieback classification modelling using high-resolution digital multispectral imagery and in situ assessments of crown condition. *Remote Sensing Letters, 3,* 541–550.

Gao, B., & Goetz, A. (1990). Column atmospheric water vapor and vegetation liquid water retrievals from airborne imaging spectrometer data. *Journal of Geophysical Research, 95,* 3549–3564.

Gao, B., Heidebrecht, K., & Goetz, A. (1993). Derivation of scaled surface reflectances from AVIRIS data. *Remote Sensing of Environment, 44,* 165–178.

Garbulsky, M.F., Peñuelas, J., Gamon, J., Inoue, Y., & Filella, I. (2011). The photochemical reflectance index (PRI) and the remote sensing of leaf, canopy and ecosystem radiation use efficiencies: A review and meta-analysis. *Remote Sensing of Environment, 115,* 281–297.

Giardino, C., Bartoli, M., Candiani, G., Bresciani, M., & Pellegrini, L. (2007a). Recent changes in macrophyte colonisation patterns: An imaging spectrometry-based evaluation of southern Lake Garda (northern Italy). *Journal of Applied Remote Sensing, 1* (011509-011509-011517).

Giardino, C., Brando, V., Dekker, A., Strömbeck, N., & Candiani, G. (2007). Assessment of water quality in Lake Garda (Italy) using Hyperion. *Remote Sensing of Environment, 109,* 183–195.

Gitelson, A. (1992). The peak near 700 nm on reflectance spectra of algae and water: Relationships of its magnitude and position with chlorophyll concentration. *International Journal of Remote Sensing, 13,* 3367–3373.

Gitelson, A., Dall'Olmo, G., Moses, W., Rundquist, D., Barrow, T., Fisher, T., et al. (2008). A simple semi-analytical model for remote estimation of chlorophyll-a in turbid waters: Validation. *Remote Sensing of Environment, 112,* 3582–3593.

Gitelson, A., & Merzlyak, M. (1996). Signature analysis of leaf reflectance spectra: Algorithm development for remote sensing of chlorophyll. *Journal of Plant Physiology, 148,* 494–500.

Gitelson, A., Schalles, J., & Hladik, C. (2007). Remote chlorophyll-a retrieval in turbid, productive estuaries: Chesapeake Bay case study. *Remote Sensing of Environment, 109,* 464–472.

Gons, H., Auer, M., & Effler, S. (2008). MERIS satellite chlorophyll mapping of oligotrophic and eutrophic waters in the Laurentian Great Lakes. *Remote Sensing of Environment, 112,* 4098–4106.

Gons, H., Hakvoort, H., Peters, S.M., & Simis, S.H. (2005). Optical detection of cyanobacterial blooms. In J. Huisman, H.P. Matthijs, & P. Visser (Eds.), *Harmful cyanobacteria* (pp. 177–199). Netherlands: Springer.

Green, R., Eastwood, M., Sarture, C., Chrien, T., Aronsson, M., Chippendale, B., et al. (1998). Imaging spectroscopy and the Airborne Visible Infrared Imaging Spectrometer (AVIRIS). *Remote Sensing of Environment, 65,* 227–248.

Hanjra, M., & Qureshi, M. (2010). Global water crisis and future food security in an era of climate change. *Food Policy, 35,* 365–377.

Hardisky, M., Gross, M., & Klemas, V. (1986). Remote sensing of coastal wetlands. *BioScience, 36,* 453–460.

Henderson, F., & Lewis, A. (2008). Radar detection of wetland ecosystems: A review. *International Journal of Remote Sensing, 29,* 5809–5835.

Hess, L., Melack, J., Novo, E., Barbosa, C., & Gastil, M. (2003). Dual-season mapping of wetland inundation and vegetation for the central Amazon basin. *Remote Sensing of Environment, 87,* 404–428.

Hestir, E., Brando, V., Campbell, G., Dekker, A., & Malthus, T. (2015). The relationship between dissolved organic matter absorption and dissolved organic carbon in reservoirs along a temperate to tropical gradient. *Remote Sensing of Environment, 156,* 395–402.

Hestir, E., Greenberg, J., & Ustin, S. (2012). Classification trees for aquatic vegetation community prediction from imaging spectroscopy. *IEEE Journal of Selected Topics in Applied Earth Observations and Remote Sensing, 5,* 1572–1584.

Hestir, E., Khanna, S., Andrew, M., Santos, M., Viers, J., Greenberg, J., et al. (2008). Identification of invasive vegetation using hyperspectral remote sensing in the California delta ecosystem. *Remote Sensing of Environment, 112,* 4034–4047.

Heumann, B. (2011). Satellite remote sensing of mangrove forests: Recent advances and future opportunities. *Progress in Physical Geography, 35,* 87–108.

Hochberg, E., Mobley, C., Park, Y., Goodman, J., Turpie, K., Gao, B., et al. (2011). *HyspIRI sunglint subgroup report.* NASA white paper, 1–72 (http://hyspiri.jpl. nasa.gov/downloads/2011_Sunglint_Report/2011_HyspIRI_Sunglint_Report_11-4.pdf).

Hoogenboom, H., Dekker, A., & Althius, I. (1998). Simulation of AVIRIS sensitivity for detecting chlorophyll over coastal and inland waters. *Remote Sensing of Environment, 65,* 333–340.

Hoogenboom, H., Dekker, A., & De Haan, J. (1998). Retrieval of chlorophyll and suspended matter from imaging spectrometry data by matrix inversion. *Canadian Journal of Remote Sensing, 24,* 144–152.

Hu, C., Feng, L., Lee, Z., Davis, C., Mannino, A., McClain, C., et al. (2012). Dynamic range and sensitivity requirements of satellite ocean color sensors: Learning from the past. *Applied Optics, 51,* 6045–6062.

Hunter, P., Tyler, A., Willby, N., & Gilvear, D. (2008). The spatial dynamics of vertical migration by *Microcystis aeruginosa* in a eutrophic shallow lake: A case study using high spatial resolution time-series airborne remote sensing. *Limnology and Oceanography, 53,* 2391–2406.

Itten, K., Dell'Endice, F., Hueni, A., Kneubühler, M., Schläpfer, D., Odermatt, D., et al. (2008). APEX — The hyperspectral ESA airborne prism experiment. *Sensors, 8,* 6235–6259.

Khanna, S., Santos, M., Hestir, E., & Ustin, S. (2012). Plant community dynamics relative to the changing distribution of a highly invasive species, *Eichhornia crassipes*: A remote sensing perspective. *Biological Invasions, 14,* 717–733.

Khanna, S., Santos, M., Ustin, S., & Haverkamp, P. (2011). An integrated approach to a biophysiologically based classification of floating aquatic macrophytes. *International Journal of Remote Sensing, 32,* 1067–1094.

Klemas, V. (2011). Remote sensing of wetlands: Case studies comparing practical techniques. *Journal of Coastal Research, 27,* 418–427.

Klemas, V. (2013a). Remote sensing of emergent and submerged wetlands: An overview. *International Journal of Remote Sensing, 34,* 6286–6320.

Klemas, V. (2013b). Using remote sensing to select and monitor wetland restoration sites: An overview. *Journal of Coastal Research, 29,* 958–970.

Klemas, V. (2014). Remote sensing of riparian and wetland buffers: An overview. *Journal of Coastal Research, 30,* 869–880.

Kutser, T. (2009). Passive optical remote sensing of cyanobacteria and other intense phytoplankton blooms in coastal and inland waters. *International Journal of Remote Sensing, 30,* 4401–4425.

Kutser, T., Herlevi, A., Kallio, K., & Arst, H. (2001). A hyperspectral model for interpretation of passive optical remote sensing data from turbid lakes. *Science of the Total Environment, 268,* 47–58.

Kutser, T., Metsamaa, L., Strömbeck, N., & Vahtmäe, E. (2006). Monitoring cyanobacterial blooms by satellite remote sensing. *Estuarine, Coastal and Shelf Science, 67,* 303–312.

Kutser, T., Pierson, D., Tranvik, L., Reinart, A., Sobek, S., & Kallio, K. (2005). Using satellite remote sensing to estimate the colored dissolved organic matter absorption coefficient in lakes. *Ecosystems, 8,* 709–720.

Kutser, T., Vahtmäe, E., & Praks, J. (2009). A sun glint correction method for hyperspectral imagery containing areas with non-negligible water leaving NIR signal. *Remote Sensing of Environment, 113,* 2267–2274.

LaCapra, V., Melack, J., Gastil, M., & Valeriano, D. (1996). Remote sensing of foliar chemistry of inundated rice with imaging spectrometry. *Remote Sensing of Environment, 55,* 50–58.

Le, C., Hu, C., Cannizzaro, J., English, D., Muller-Karger, F., & Lee, Z. (2013). Evaluation of chlorophyll-a remote sensing algorithms for an optically complex estuary. *Remote Sensing of Environment, 129,* 75–89.

Lee, Z., Carder, K., Arnone, R., & He, M. (2007). Determination of primary spectral bands for remote sensing of aquatic environments. *Sensors, 7,* 3428–3441.

Lee, Z., Shang, S., Hu, C., & Zibordi, G. (2014). Spectral interdependence of remote-sensing reflectance and its implications on the design of ocean color satellites. *Applied Optics, 53,* 3301–3310.

Legleiter, C., & Roberts, D. (2005). Effects of channel morphology and sensor spatial resolution on image-derived depth estimates. *Remote Sensing of Environment, 95,* 231–247.

Legleiter, C., & Roberts, D. (2009). A forward image model for passive optical remote sensing of river bathymetry. *Remote Sensing of Environment, 113,* 1025–1045.

Legleiter, C., Roberts, D., Marcus, W., & Fonstad, M. (2004). Optical remote sensing of river channel morphology and in-stream habitat: Physical basis and feasibility. *Remote Sensing of Environment, 93,* 493–510.

Lindell, T., Pierson, D., Premazzi, G., & Zilioli, E. (1999). Manual for monitoring European lakes using remote sensing techniques. *EUR Report n. 18665 EN.* Luxembourg: Office for Official Publications of the European Communities.

Liu, X., Zhang, Y., Yin, Y., Wang, M., & Qin, B. (2013). Wind and submerged aquatic vegetation influence bio-optical properties in large shallow Lake Taihu, China. *Journal of Geophysical Research, Biogeosciences, 118,* 713–727.

Lulla, K. (1983). The Landsat satellites and selected aspects of physical geography. *Progress in Physical Geography, 7,* 1–45.

Mackay, A., Davidson, T., Wolski, P., Woodward, S., Mazebedi, R., Masamba, W., et al. (2012). Diatom sensitivity to hydrological and nutrient variability in a subtropical, flood-pulse wetland. *Ecohydrology, 5,* 491–502.

Matthews, M. (2011). A current review of empirical procedures of remote sensing in in-land and near-coastal transitional waters. *International Journal of Remote Sensing, 32*, 6855–6899.

McCullough, I., Loftin, C., & Sader, S. (2012). High-frequency remote monitoring of large lakes with MODIS 500 m imagery. *Remote Sensing of Environment, 124*, 234–241.

McFeeters, S. (1996). The use of the normalized difference water index (NDWI) in the de-lineation of open water features. *International Journal of Remote Sensing, 17*, 1425–1432.

Meerhoff, M., Mazzeo, N., Moss, B., & Rodríguez-Gallego, L. (2003). The structuring role of free-floating versus submerged plants in a subtropical shallow lake. *Aquatic Ecology, 37*, 377–391.

Melack, J. (2004). Remote sensing of tropical wetlands. In S. Ustin (Ed.), *Manual of remote sensing. Remote sensing for natural resources management and environmental monitoring, Vol. 4.* (pp. 319–343). New York: Wiley.

Mercury, M., Green, R., Hook, S., Oaida, B., Wu, W., Gunderson, A., et al. (2012). Global cloud cover for assessment of optical satellite observation opportunities: A HysplRI case study. *Remote Sensing of Environment, 126*, 62–71.

Mertes, L. (2002). Remote sensing of riverine landscapes. *Freshwater Biology, 47*, 799–816.

Mertes, L., & Warrick, J. (2001). Measuring flood output from 110 coastal watersheds in California with field measurements and SeaWiFS. *Geology, 29*, 659–662.

Mitsch, W., Bernal, B., Nahlik, A., Mander, Ü., Zhang, L., Anderson, C., et al. (2013). Wet-lands, carbon and climate change. *Landscape Ecology, 28*, 583–597.

Mouw, C., Greb, S., Aurin, D., DiGiacomo, P., Lee, Z., Twardowski, M., et al. (2015). Aquatic color radiometry remote sensing of coastal and inland waters: Challenges and recom-mendations for future satellite missions. *Remote Sensing of Environment, 160*, 15–30.

Muller, E., DÉCamps, H., & Dobson, M. (1993). Contribution of space remote sensing to river studies. *Freshwater Biology, 29*, 301–312.

Munyati, C. (2000). Wetland change detection on the Kafue Flats, Zambia, by classification of a multitemporal remote sensing image dataset. *International Journal of Remote Sensing, 21*, 1787–1806.

Nair, A., Sathyendranath, S., Platt, T., Morales, J., Stuart, V., Forget, M., et al. (2008). Remote sensing of phytoplankton functional types. *Remote Sensing of Environment, 112*, 3366–3375.

National Research Council (2007). *Earth science and applications from space: National im-peratives for the next decade and beyond.* Washington, D.C.: The National Academic Press.

Nelson, S., Soranno, P., Cheruvelil, K., Batzli, S., & Skole, D. (2003). Regional assessment of lake water clarity using satellite remote sensing. *Journal of Limnology, 62*, 27–32.

Odermatt, D., Gitelson, A., Brando, V., & Schaepman, M. (2012). Review of constituent re-trieval in optically deep and complex waters from satellite imagery. *Remote Sensing of Environment, 118*, 116–126.

Ogashawara, I., Mishra, D., Mishra, S., Curtarelli, M., & Stech, J. (2013). A performance re-view of reflectance based algorithms for predicting phycocyanin concentrations in in-land waters. *Remote Sensing, 5*, 4774–4798.

Olmanson, L., Brezonik, P., & Bauer, M. (2014). Geospatial and temporal analysis of a 20-year record of Landsat-based water clarity in Minnesota's 10,000 lakes. *Journal of the American Water Resources Association, 50*, 748–761.

O'Reilly, J., Maritorena, S., Mitchell, B., Siegel, D., Carder, K., Garver, S., et al. (1998). Ocean color chlorophyll algorithms for SeaWiFS. *Journal of Geophysical Research, Oceans, 103*, 24937–24953.

Ozesmi, S., & Bauer, M. (2002). Satellite remote sensing of wetlands. *Wetlands Ecology and Management, 10*, 381–402.

Paerl, H. (2008). Nutrient and other environmental controls of harmful cyanobacterial blooms along the freshwater–marine continuum. In H.K. Hudnell (Ed.), *Cyanobacterial harmful algal blooms: State of the science and research needs* (pp. 217–237). New York: Springer.

Peñuelas, J., Gamon, J.A., Griffin, K., & Field, C. (1993). Assessing community type, plant biomass, pigment composition, and photosynthetic efficiency of aquatic vegetation from spectral reflectance. *Remote Sensing of Environment, 46*, 110–118.

Pierson, D., & Strömbeck, N. (2001). Estimation of radiance reflectance and the concentra-tions of optically active substances in Lake Mälaren, Sweden, based on direct and in-verse solutions of a simple model. *Science of the Total Environment, 268*, 171–188.

Pinardi, M., Bartoli, M., Longhi, D., & Viaroli, P. (2011). Net autotrophy in a fluvial lake: The relative role of phytoplankton and floating-leaved macrophytes. *Aquatic Sciences, 73*, 389–403.

Poulin, B., Davranche, A., & Lefebvre, G. (2010). Ecological assessment of *Phragmites australis* wetlands using multi-season SPOT-5 scenes. *Remote Sensing of Environment, 114*, 1602–1609.

Prigent, C., Matthews, E., Aires, F., & Rossow, W. (2001). Remote sensing of global wetland dynamics with multiple satellite data sets. *Geophysical Research Letters, 28*, 4631–4634.

Ramsey, E., & Rangoonwala, A. (2011). Remote sensing of wetland vegetation focusing on hyperspectral mapping. In P. Thenkabail, D. Lyon, & A. Huete (Eds.), *Hyperspectral re-mote sensing of vegetation* (pp. 487–512). Boca Raton: CRC Press.

Raymond, P., Hartmann, J., Lauerwald, R., Sobek, S., McDonald, C., Hoover, M., et al. (2013). Global carbon dioxide emissions from inland waters. *Nature, 503*, 355–359.

Rebelo, L., Finlayson, C., & Nagabhatla, N. (2009). Remote sensing and GIS for wetland in-ventory, mapping and change analysis. *Journal of Environmental Management, 90*, 2144–2153.

Reynolds, C., Oliver, R., & Walsby, A. (1987). Cyanobacterial dominance: The role of buoy-ancy regulation in dynamic lake environments. *New Zealand Journal of Marine and Freshwater Research, 21*, 379–390.

Richardson, A., Duigan, S., & Berlyn, G. (2002). An evaluation of noninvasive methods to estimate foliar chlorophyll content. *New Phytologist, 153*, 185–194.

Richter, R., & Schläpfer, D. (2011). *Atmospheric/topographic correction for satellite imagery.* Wessling, Germany: DLR, 202.

Rocchini, D., Balkenhol, N., Carter, G., Foody, G., Gillespie, T., He, K., et al. (2010). Remotely sensed spectral heterogeneity as a proxy for species diversity: Recent advances and open challenges. *Ecological Informatics, 5*, 318–329.

Rosso, P., Ustin, S., & Hastings, A. (2005). Mapping marshland vegetation of San Francisco Bay, California, using hyperspectral data. *International Journal of Remote Sensing, 26*, 5169–5191.

Rundquist, D., Narumalani, S., & Narayanan, R. (2001). A review of wetlands remote sens-ing and defining new considerations. *Remote Sensing Reviews, 20*, 207–226.

Santos, M., Anderson, L., & Ustin, S. (2011). Effects of invasive species on plant communi-ties: An example using submersed aquatic plants at the regional scale. *Biological Invasions, 13*, 443–457.

Santos, M., Hestir, E., Khanna, S., & Ustin, S. (2012). Image spectroscopy and stable iso-topes elucidate functional dissimilarity between native and nonnative plant species in the aquatic environment. *New Phytologist, 193*, 683–695.

Santos, M., Khanna, S., Hestir, E., Andrew, M., Rajapakse, S., Greenberg, J., et al. (2009). Use of hyperspectral remote sensing to evaluate efficacy of aquatic plant management. *Invasive Plant Science and Management, 2*, 216–229.

Schaeffer, B., Schaeffer, K., Keith, D., Lunetta, R., Conmy, R., & Gould, R. (2013). Barriers to adopting satellite remote sensing for water quality management. *International Journal of Remote Sensing, 34*, 7534–7544.

Schaepman, M., Ustin, S., Plaza, A., Painter, T., Verrelst, J., & Liang, S. (2009). Earth system science related imaging spectroscopy—An assessment. *Remote Sensing of Environment, 113*(Supplement 1), S123–S137.

Schmidt, K., & Skidmore, A. (2003). Spectral discrimination of vegetation types in a coastal wetland. *Remote Sensing of Environment, 85*, 92–108.

Siegel, D., Maritorena, S., Nelson, N., Behrenfeld, M., & McClain, C. (2005). Colored dis-solved organic matter and its influence on the satellite-based characterization of the ocean biosphere. *Geophysical Research Letters, 32*, L20605.

Silva, T., Costa, M., & Melack, J. (2010). Spatio-temporal variability of macrophyte cover and productivity in the eastern Amazon floodplain: A remote sensing approach. *Remote Sensing of Environment, 114*, 1998–2010.

Silva, T., Costa, M., Melack, J., & Novo, E. (2008). Remote sensing of aquatic vegetation: Theory and applications. *Environmental Monitoring and Assessment, 140*, 131–145.

Simis, S., Peters, S., & Gons, H. (2005). Remote sensing of the cyanobacterial pigment phy-cocyanin in turbid inland water. *Limnology and Oceanography, 50*, 237–245.

Sims, D., & Gamon, J. (2002). Relationships between leaf pigment content and spectral re-flectance across a wide range of species, leaf structures and developmental stages. *Remote Sensing of Environment, 81*, 337–354.

Song, C., Xu, X., Tian, H., & Wang, Y. (2009). Ecosystem–atmosphere exchange of $CH_4$ and $N_2O$ and ecosystem respiration in wetlands in the Sanjiang Plain, Northeastern China. *Global Change Biology, 15*, 692–705.

Stendera, S., Adrian, R., Bonada, N., Cañedo-Argüelles, M., Hugueny, B., Januschke, K., et al. (2012). Drivers and stressors of freshwater biodiversity patterns across different eco-systems and scales: A review. *Hydrobiologia, 696*, 1–28.

Stomp, M., Huisman, J., de Jongh, F., Veraart, A., Gerla, D., Rijkeboer, M., et al. (2004). Adaptive divergence in pigment composition promotes phytoplankton biodiversity. *Nature, 432*, 104–107.

Striebel, M., Behl, S., Diehl, S., & Stibor, H. (2009). Spectral niche complementarity and car-bon dynamics in pelagic ecosystems. *The American Naturalist, 174*, 141–147.

Strong, A. (1974). Remote sensing of algal blooms by aircraft and satellite in Lake Erie and Utah Lake. *Remote Sensing of Environment, 3*, 99–107.

Strozzi, T., Wiesmann, A., Kääb, A., Joshi, S., & Mool, P. (2012). Glacial lake mapping with very high resolution satellite SAR data. *Natural Hazards and Earth System Science, 12*, 2487–2498.

Thiemann, S., & Kaufmann, H. (2002). Lake water quality monitoring using hyperspectral airborne data—A semiempirical multisensor and multitemporal approach for the Mecklenburg Lake District, Germany. *Remote Sensing of Environment, 81*, 228–237.

Thompson, D., Gao, B., Green, R., Roberts, D., Dennison, P., & Lundeen, S. (2015). Atmo-spheric correction for global mapping spectroscopy: ATREM advances for the HysplRI preparatory campaign. *Remote Sensing of Environment, 167*, 64–77.

Tranvik, L., Downing, J., Cotner, J., Loiselle, S., Striegle, R., Ballatore, T., et al. (2009). Lakes and reservoirs as regulators of carbon cycling and climate. *Limnology and Oceanography, 54*, 2298–2314.

Turpie, K. (2013). Explaining the spectral red-edge features of inundated marsh vegeta-tion. *Journal of Coastal Research, 29*, 1111–1117.

Underwood, E., Mulitsch, M., Greenberg, J., Whiting, M., Ustin, S., & Kefauver, S. (2006). Mapping invasive aquatic vegetation in the Sacramento–San Joaquin delta using hyperspectral imagery. *Environmental Monitoring and Assessment, 121*, 47–64.

Ustin, S. (2013). Remote sensing of canopy chemistry. *Proceedings of the National Academy of Sciences, 110*, 804–805.

Ustin, S., & Gamon, J. (2010). Remote sensing of plant functional types. *New Phytologist, 186*, 795–816.

Ustin, S., Gitelson, A., Jacquemoud, S., Schaepman, M., Asner, G., Gamon, J., et al. (2009). Retrieval of foliar information about plant pigment systems from high resolution spectroscopy. *Remote Sensing of Environment, 113*(Supplement 1), S67–S77.

Ustin, S., Roberts, D., Gamon, J., Asner, G., & Green, R. (2004). Using imaging spectroscopy to study ecosystem processes and properties. *BioScience, 54*, 523–534.

Vanderbilt, V.C., Khanna, S., & Ustin, S.L. (2007). Impact of pixel size on mapping surface water in subsolar imagery. *Remote Sensing of Environment, 109*, 1–9.

Vanderstukken, M., Declerck, S., Decaestecker, E., & Muylaert, K. (2014). Long-term allelo-pathic control of phytoplankton by the submerged macrophyte *Elodea nuttallii*. *Freshwater Biology, 59*, 930–941.

Vanhellemont, Q., & Ruddick, K. (2014). Turbid wakes associated with offshore wind tur-bines observed with Landsat 8. *Remote Sensing of Environment, 145*, 105–115.

Villa, P., Bresciani, M., Braga, F., & Bolpagni, R. (2014). Comparative assessment of broadband vegetation indices over aquatic vegetation. *IEEE Journal of Selected Topics in Applied Earth Observations and Remote Sensing, 7*, 3117–3127.

Villa, P., Laini, A., Bresciani, M., & Bolpagni, R. (2013). A remote sensing approach to monitor the conservation status of lacustrine *Phragmites australis* beds. *Wetlands Ecology and Management, 21*, 399–416.

Villa, P., Mousivand, A., & Bresciani, M. (2014). Aquatic vegetation indices assessment through radiative transfer modeling and linear mixture simulation. *International Journal of Applied Earth Observation and Geoinformation, 30*, 113–127.

Vincent, R., Qin, X., McKay, R., Miner, J., Czajkowski, K., Savino, J., et al. (2004). Phycocyanin detection from LANDSAT TM data for mapping cyanobacterial blooms in Lake Erie. *Remote Sensing of Environment, 89*, 381–392.

Wettle, M., Brando, V., & Dekker, A. (2004). A methodology for retrieval of environmental noise equivalent spectra applied to four Hyperion scenes of the same tropical coral reef. *Remote Sensing of Environment, 93*, 188–197.

Wickland, D. (1989). Future directions for remote sensing in terrestrial ecological research. In G. Asrar (Ed.), *Theory and applications of optical remote sensing* (pp. 752). New York: Wiley.

Woodward, G., Perkins, D., & Brown, L. (2010). Climate change and freshwater ecosystems: Impacts across multiple levels of organization. *Philosophical Transactions of the Royal Society, B: Biological Sciences, 365*, 2093–2106.

Wulder, M., Masek, J., Cohen, W., Loveland, T., & Woodcock, C. (2012). Opening the archive: How free data has enabled the science and monitoring promise of Landsat. *Remote Sensing of Environment, 122*, 2–10.

Zhou, L., & Zhou, G. (2009). Measurement and modelling of evapotranspiration over a reed (*Phragmites australis*) marsh in Northeast China. *Journal of Hydrology, 372*, 41–47.

Zhu, W., Yu, Q., Tian, Y., Becker, B., Zheng, T., & Carrick, H. (2014). An assessment of remote sensing algorithms for colored dissolved organic matter in complex freshwater environments. *Remote Sensing of Environment, 140*, 766–778.

Zomer, R., Trabucco, A., & Ustin, S. (2009). Building spectral libraries for wetlands land cover classification and hyperspectral remote sensing. *Journal of Environmental Management, 90*, 2170–2177.